

Pyrrolizidine alkaloids: occurrence, biology, and chemical synthesis

Jeremy Robertson* and Kiri Stevens

 Received 00th January 20xx,
Accepted 00th January 20xx

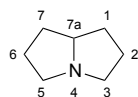
DOI: 10.1039/x0xx00000x

www.rsc.org/

This review summarises the pyrrolizidine literature from January 2013 to December 2015. Coverage includes: the isolation and structure of new pyrrolizidines; pyrrolizidine biosynthesis; biological activity, including the occurrence of pyrrolizidines as toxic components or contaminants in foods and beverages; and formal and total syntheses of naturally-occurring pyrrolizidine alkaloids and closely related non-natural analogues.

Introduction

This review concerns chemical, biological, and environmental aspects of the class of pyrrolizidine alkaloids (PAs); natural products and their close structural analogues (mainly stereoisomers) that contain the pyrrolizidine motif, as shown below with the conventional atom numbering indicated.



The coverage picks up from where our previous review¹ left off and encompasses the literature published up to the end of December 2015.

During this three-year period our knowledge of the broader chemistry and biology of PAs and their place in the environment has advanced substantially on several fronts. For example, although the field of PA research originated when the symptoms of poisoning were associated with the ingestion by humans and domestic animals of certain plants, the details of how toxicity arises remains an area of active investigation. Recently, the molecular mechanisms involved in PA-induced toxicity have become more refined through both computation, to understand the origin of toxic dehydropyrrolizidines, and by experiment, to determine the fate *in vivo* of reactive iminium ions derived from them. A second major recent advance is the elucidation of the biosynthetic pathways leading to bacterial pyrrolizidines of the vinylogous urethane type. This work has led to the identification of new members of this class and a prediction based on genetic relationships that many more PAs will be discovered by further examining the metabolite profiles of diverse bacterial species. These aspects are outlined in the

first part of the review which also includes a summary of the large research effort to confirm the presence of and quantify toxic PAs in foods, beverages, and medicinal formulations, which has obvious implications for human health.

The second part of the review highlights the fascination that these alkaloids continue to hold for synthetic chemists who are attracted by the biological activity and, being relatively simple in structure, the opportunities for developing, testing, and showcasing new synthetic methods. The majority of these targets contain a hydroxymethyl substituent, most commonly at C(1) or C(3), but coverage extends to simple polyhydroxypyrrolizidines, aminopyrrolizidines, and more exotic structures that contain the pyrrolizidine fragment. Compounds in which the pyrrolizidine is the minor structural feature or which have been deemed by the authors to be of lesser interest are not covered.

This survey of the synthetic chemistry shows that some genuinely new strategies have emerged for application to PAs. There has been a reduced focus on enantiospecific syntheses from chiral pool materials, an increase in convergent approaches, and new methods for stereoselective C–C and C–N bond construction including the exploitation of two relatively recent additions to the synthetic chemist's toolbox: asymmetric organocatalysis and C–H activation. Coverage includes essentially all the reported total and formal syntheses but where particular methodologies or strategies were described in the previous review, discussion is kept to a minimum. As in the previous review, the syntheses are mainly described chronologically within each sub-section except where an alternative grouping provides a more natural flow of the discussion (e.g. routes based on nitron chemistry).

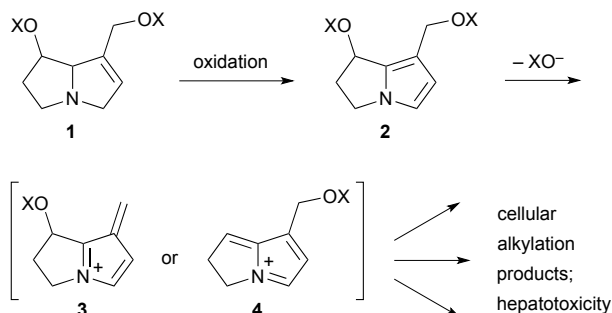
Non-synthetic aspects

Metabolism and toxicity

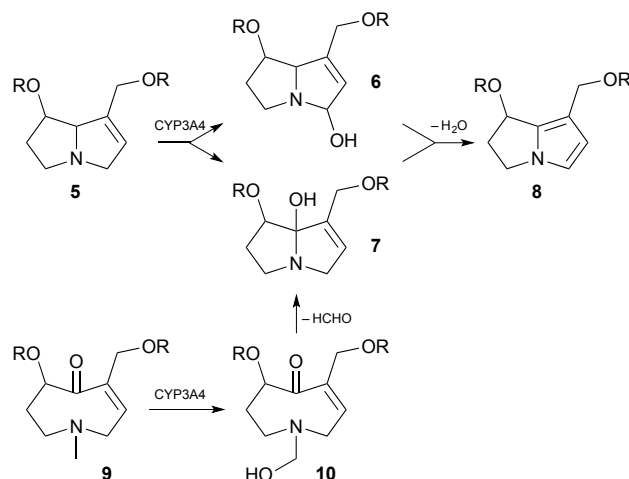
Hepatotoxicity (especially veno-occlusive disease) is a potentially serious result of ingestion of PAs. Following

Department of Chemistry, Chemistry Research Laboratory, University of Oxford, Mansfield Road, Oxford, OX1 3TA, UK. E-mail: jeremy.robertson@chem.ox.ac.uk; Tel: +44 (0)1865275660.

ingestion, those PAs that bear a C(1)–C(2) double bond may become metabolised to pyrrolizidine intermediates **2** (Scheme 1) which then rapidly eject a carboxylate leaving group from either the C(1)-hydroxymethyl or C(7) oxy-substituents giving extended iminium ions **3** or **4**, respectively. Such iminium intermediates are reactive alkylating agents that are readily trapped by cellular components leading ultimately to acute liver damage and, in some animal models, genotoxicity and carcinogenesis.



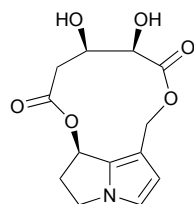
Work has continued in order to gain insight into each step of this general scheme. With reference to the first step ('oxidation', Scheme 1), application of the electrophilic Fukui function was combined with computed bond dissociation energies and molecular docking simulations to predict the initial site of human cytochrome P450 (CYP3A4) mediated activation of toxic pyrrolizidines of the heliotrine, retronecine, and otonecine classes.² As might be expected, the C(3)-, C(5)- and C(7a)- [numbered C(8) in the paper] positions in the first two classes, and the C(3)-, C(5)- and *N*-methyl sites in the otonecines were shown to be the most susceptible by the first two measures; molecular docking results showed more variation between the three classes. On this basis, the authors presented three hydroxylation mechanisms (Scheme 2): hydrogen abstraction and rebound hydroxylation at C(3)- (\rightarrow **6**) or C(7a)- (\rightarrow **7**) followed by dehydration (\rightarrow **8**); or, for the otonecines **9**, demethylation by hydroxylation (\rightarrow **10**) and loss of formaldehyde that leads, following transannular cyclisation, to the same type of C(7a)-hydroxypyrrolizidine intermediate **7** obtained from the heliotrine/retronecine classes. Representatives of the three classes – lasiocarpine, retrorsine, and senkirkine – were then incubated with either human CYP3A4 or human liver microsomes, in both cases trapping the dehydropyrrolizidines with glutathione (GSH). The rate of formation of the mono-GSH adduct in both *in vitro* studies was highest for lasiocarpine ($k_{\text{rel}} = 19$), then retrorsine ($k_{\text{rel}} = 7.6$) and senkirkine ($k_{\text{rel}} = 1$).



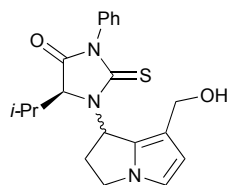
Scheme 2 Formation of dehydropyrrolizidines by cytochrome P450-mediated hydroxylation and dehydration, with oxidative demethylation in the otonecine series.

A further study examined the metabolic profile of lasiocarpine when exposed to liver microsomes from human, pig, rat, mouse, rabbit, and sheep.³ The study found that the distribution of twelve metabolites was broadly similar in the non-human cases. With human liver microsomes, while the same major metabolite, M9, was produced, the product of *O*-demethylation, a second metabolite, M7, was formed to almost the same extent. Comparisons were carried out with recombinant human CYP3A4 to support the involvement of the CYP3A enzyme family in lasiocarpine metabolism. The results are interpreted in relation to the relative toxicity of PAs in different mammalian species.

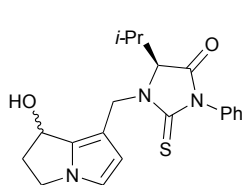
With reference to the second step (' XO^- ') in Scheme 1, and building on the synthesis of standards DHP-dG-3, DHP-dG-4, DHP-dA-3, and DHP-dA-4,⁴ Fu's group showed that all four adducts were produced in the livers of rats dosed with hepatotoxic PAs (riddelliine and its *N*-oxide, retrorsine, monocrotaline, lasiocarpine, heliotrine, clivorine, and senkirkine).⁵ For non-hepatotoxic alkaloids, and within the limits of detection, these adducts were either present at very low concentrations (lycopsamine) or absent (retronecine, platyphilline). The authors concluded that the four adducts act as a biomarker for PA-induced tumour formation. In related work, the group add to knowledge of how toxic PAs interact with cellular constituents following activation to the dehydro-forms.⁶ In this study, dehydromonocrotaline **11** was treated with valine to yield four adducts, characterised as their phenylisothiocyanate (PITC) adducts **12/13** and **14/15**.



11, dehydromonocrotaline

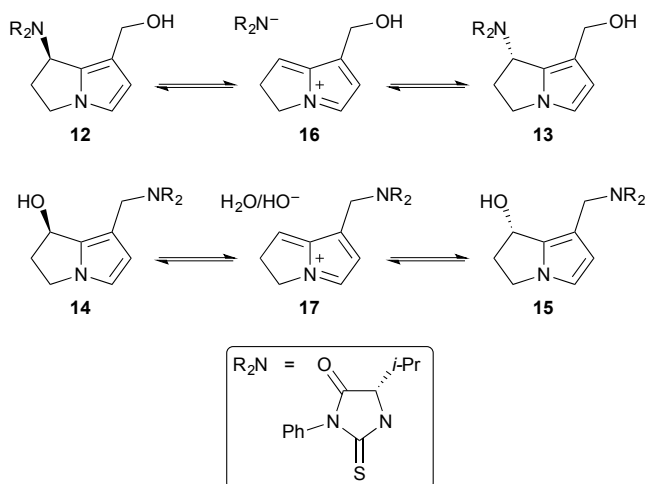


12,13

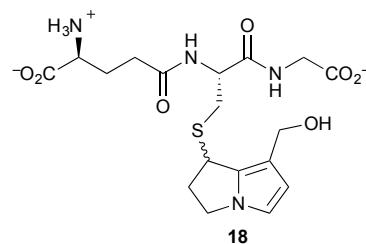


14,15

The group then prepared these adducts discretely and studied the mechanism of interconversion of epimeric pairs **12/13** and **14/15** in ^{18}O -labelled water.⁷ The equilibration of **12** and **13** (Scheme 3) was accompanied by incorporation of ^{18}OH into the C(1)-hydroxymethyl substituent whereas the equilibration of **14** and **15** (and thence the C(7)- ^{18}OH derivatives) did not, apparently, lead to hydrolysis of the C(1)- CH_2NR_2 group.

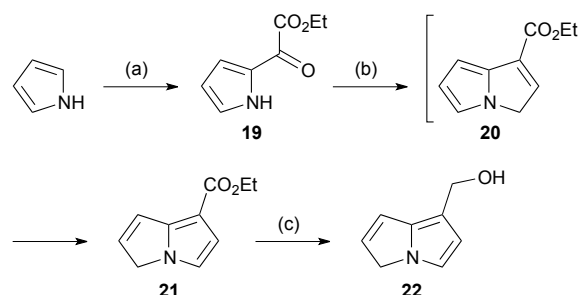
Scheme 3 $\text{S}_{\text{N}}1$ -type equilibration of DHP-valine-PITC adducts.

To shed further light on potential metabolic pathways of toxic pyrrolizidines, incubation of dehydromonocrotaline **11** with a sub-stoichiometric quantity of glutathione (GSH) in the presence of spleen phosphodiesterase gave the C(7)-GS adduct **18**; use of a large excess of GSH gave the C(7,9)-bis-GS adduct (not shown).⁸ Shaking **18** with either 2'-deoxyguanosine (dG) or 2'-deoxyadenosine (dA) produced all four mono-adducts in both series, DHP-dG-1–4 or DHP-dA-1–4, over a period of hours to days. Similar reactions with the C(7,9)-bis-GS adduct resulted in, at most, traces of these mono-adducts. It is concluded that the conjugation of dehydropyrrolizidines (DHPs) with glutathione is not, as was previously considered, a detoxification pathway; indeed, the C(7)-GS adducts are proposed as a relatively stable 'reservoir' of the DHPs themselves.



18

In the same context, oxidative degradation of hepatotoxic PAs, such as retrorsine, by human liver microsomes (or in an electrochemical cell) gave a variety of dehydropyrrolizidines, among which the novel metabolite **22** (Scheme 4) was observed.⁹ The structure of this compound was confirmed by comparison with an authentic synthetic sample, prepared from pyrrole as shown. In the presence of glutathione (GSH), this metabolite and a minor alkene regioisomer formed GSH adducts (*cf.* **18**) most likely *via* protonation at C(6) and subsequent trapping of the so-formed extended iminium ion.

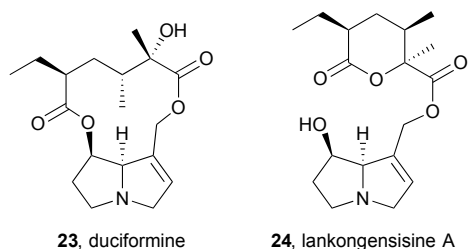
Scheme 4 Reagents and conditions: (a) ethoxalyl chloride, pyridine, CH_2Cl_2 , -80°C ; (b) NaH, vinyl triphenylphosphonium bromide, Et_2O , reflux; (c) LiAlH_4 , Et_2O , reflux.

Stegemeier developed an *in vitro* cell model to take up and activate dehydropyrrolizidine alkaloids and their *N*-oxides in order to arrive at a toxicity ranking of small quantities of these molecules present in a variety of samples.¹⁰ It was found, in a pilot study, that chicken hepatocellular carcinoma (CRL-2118) cells are highly susceptible to exposure to riddelliine and these, in combination with a 3-(4,5-dimethylthiazol-2-yl)-2,5-diphenyltetrazolium bromide (MTT) assay, were used to rank the toxicity of eleven pyrrolizidines. Three groups were identified: (1) highly toxic – lasiocarpine, seneciophylline, senecionine, and heliotrine; (2) moderately toxic – riddelliine, monocrotaline, and riddelliine *N*-oxide; (3) least toxic – intermedine, lycopsamine, lasiocarpine *N*-oxide, and senecionine *N*-oxide.

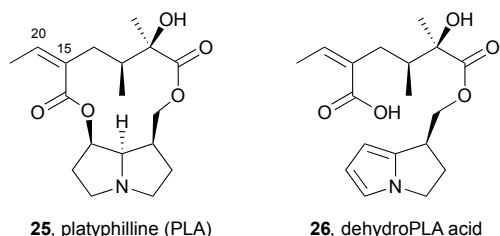
A combined metabolomic and genomic study of senecionine toxicity in rats demonstrated that the observed toxicity is associated with compromised bile acid metabolism through a series of interconnected pathways.¹¹ The paper's introduction contains a concise overview of the global impact of toxic pyrrolizidines on human health (see below).

A continuation of an investigation into the rat liver microsomal metabolism of PAs from *Ligularia duciformis* (Asteraceae) showed that 12-*O*-acetylduciformine gave both the deacetyl parent **23** and the product **24** of intramolecular

transacylation (lankongensisine A; δ -lactone stereochemistry assumed from duciformine).¹²



PAs of the platynecine type, lacking C(1–2) unsaturation, are non-toxic. Lin *et al.* showed that platyphilline **25**, a representative alkaloid of this type, is metabolised primarily to the ‘dehydroPLA acid’ **26** shown. Although containing a pyrrole, this metabolite lacks a mechanism for incorporation of a cellular nucleophile *via* ejection of a suitable leaving group; in addition, the carboxylic acid renders the metabolite relatively water-soluble and readily excreted.¹³ Minor metabolites included platyphilline *N*-oxide and the C(15–20) epoxide.



Estimation in foods etc

In parallel to trying to understand the toxicity mechanisms of PAs following ingestion, much research has been performed to improve the sensitivity and reliability of analytical techniques that can rapidly quantify the levels of toxic PAs in the complex matrices of foodstuffs, supplements, traditional medicines, and other products with which human or animal populations may come into contact. In parallel, there is a developing consensus on the likely dangerous acute and chronic exposure levels. Even within the three-year period under review, many publications have described such studies, with focus on a particular analytical technique, a particular carrier, or a particular location/source. The area has been reviewed¹⁴ and The Federal Institute for Risk Assessment (BfR) has issued an informative opinion article with a summary of the existing maximum recommended exposure levels.¹⁵

For example, reports have described the detection of toxic PAs in honey^{16,17,18,19,20,21,22,23,24} and their persistence through fermentation into mead;²⁵ in medicinal or culinary herbs^{26,27,28,29,30} and herbal or medicinal teas;^{31,32,33,34,35,36,37} in seed oils for cooking, food supplements, and cosmetics;^{38,39} and in a variety of other sources.^{40,41} Reports that PAs can persist in contaminated plant-based cattle feed even following ensiling are of potential concern when such PAs pass into milk-producing animals.^{42,43,44}

The vast majority of analyses are performed by MS and MS/MS protocols usually following pre-processing, derivatisation, or HPLC separation. A comparison of the results provided by 12 analytical laboratories on contaminated animal feed samples showed that an LC-MS/MS method seemed to offer the most consistent results but that there was sufficient variation between the laboratories to point to the need for further development of accurate analytical procedures and tools.^{45,46,47,48} The author of a separate study tabulated multiple reaction monitoring (MRM) mass spectrometric ion responses of 26 pyrrolizidine ions to highlight the difficulty of quantifying the levels of toxic PA constituents in laboratory samples of, for example, food products and they advocate quantitative NMR as a more reliable means of obtaining meaningful values.⁴⁹

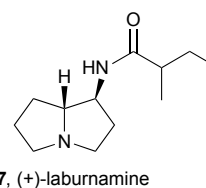
These studies highlight an emerging recognition of chronic toxicity associated with herbal teas, largely because the consumers are potentially exposed to low toxic PA levels for many years. Wide variations in toxic PA levels were recorded; for example, in a study of herbal teas available to the Swiss market,³² more than one PA was found in 50 of 70 teas studied, of which 24 were at levels above the limit of quantification, and 9 had a Margin of Exposure below 10,000 (an MOE >10,000 is deemed to pose little risk).

In each case, the sources of the contamination vary, but may include occasional (and variable) co-harvesting of toxic PA-containing species, mis-identification of the herb or plant material, contamination during processing, storage, or transport, or insufficient separation of toxic PAs in the case of seed oils.

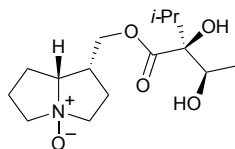
Useful bioactivity

PAs are not all toxic; many are non-toxic, for reasons alluded to above, and some exhibit potentially useful biological activity. Reports of such activity are relatively scarce but researchers will find only what they assay for; therefore, the few reported ‘hits’ may represent the tip of the iceberg of potential activity that would be revealed by assays against a wider-ranging variety of targets and cell types.

During a study of the activity of potential nicotinic ligands prepared from cytosine obtained from *Laburnum anagyroides* (Fabaceae), (+)-laburnamine **27** was isolated in sufficient quantity to enable a preliminary pharmacological evaluation.⁵⁰ The authors found that this alkaloid is a selective ligand for the rat cortical $\alpha 4/\beta 2$ neuronal nicotinic acetylcholine receptor subtype ($K_i = 0.293 \mu\text{M}$) relative to human transfected $\alpha 3/\beta 4$ ($K_i = 37 \mu\text{M}$) and rat hippocampus $\alpha 7$ ($K_i = 40 \mu\text{M}$) subtypes. A further study, on the ability of **27** to induce dopamine release relative to nicotine, indicated that (+)-laburnamine acts as a partial agonist.

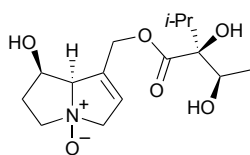


Ten known pyrrolizidines were isolated from *Rindera umbellata* (Boraginaceae). The distribution of these ten alkaloids varied substantially depending on harvest date (Jun 2007, May 2008, July 2009) and plant part (aerial parts, roots, seeds).⁵¹ The most abundant pyrrolizidine, lindelofine *N*-oxide **28**, was evaluated for its ability to promote tubulin polymerisation; the obtained $IC_{50} = 91 \mu M$ compares to $2.4 \mu M$ for paclitaxel. The authors suggest that this is the first report of the effect of a PA on tubulin polymerisation.



28, lindelofine *N*-oxide

Indicine *N*-oxide **29** (INO) is cytotoxic against a variety of tumour cell lines and has been evaluated in the clinic for the treatment of leukaemia but was withdrawn from trials due to its severe toxicity. Rathinasamy reported⁵² on the mechanism underlying this alkaloid's toxicity and found that: (1) INO blocks the cell cycle at mitosis; (2) INO causes spindle abnormalities at the IC_{50} ($\sim 100 \mu M$) while at $300 \mu M$ it depolymerises both interphase and spindle microtubules; (3) INO appears to interact with a single binding site on tubulin and this site is not the colchicine binding site; (4) INO leads to DNA cleavage following (computationally predicted) binding at the minor groove.



29, indicine *N*-oxide

Monocrotaline is cytotoxic towards HepG2 cells ($IC_{50} = 25 \mu g/mL$) and genotoxic at $\sim 50 \mu g/mL$.⁵³

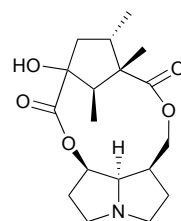
Among fourteen iminosugars isolated from *Castanospermum australe* (Fabaceae), five tetrahydroxylated pyrrolizidines (australine and epimers) were identified.⁵⁴ Four of these, along with other iminosugars, were evaluated for glycosidase inhibition and only australine showed significant activity ($IC_{50} 26\text{--}665 \mu M$ against seven different glycosidases).

Novel PAs and biosynthetic aspects

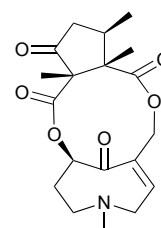
Plant PAs

In the previous review the novel cyclopentane-1,3-dicarboxylic acid linked pyrrolizidine lankongensisine **30** was described; subsequently, a related structure **31**, with a cyclopentane-1,2-dicarboxylate linkage, has been assigned to a new otonecine pyrrolizidine isolated from *Crotalaria vitellina* Ker Gawl (Fabaceae).⁵⁵ Ethanol extraction of 500 g of the dried fruits of this plant and purification of the residue gave 32 mg of (+)-crotavitalin that was characterised by a combination of NMR spectroscopy and mass spectrometry. An outline biosynthesis

of the necic acid portion of the molecule was proposed, from two molecules of isoleucine.

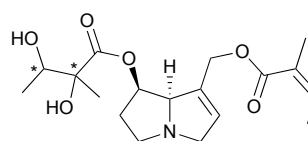


30, lankongensisine

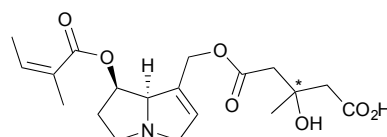


31, (+)-crotavitalin

Investigations of the alkaloidal principal components of plant species following toxicity events in cattle has led to the identification of new pyrrolizidines cryptanthine **32** and echiuplateine **33**.⁵⁶ Thus, samples of *Cryptantha inequata* and *C. utahensis* (Boraginaceae) were collected opportunistically following a hepatotoxicity incident in the Kingman area of Arizona, USA, and alkaloid profiles established by HPLC-ESI-MS. For the *C. utahensis* extract, the major peak (corresponding to cryptanthine, $0.55 \pm 0.04 \text{ mg/g}$ dry weight of plant) was not correlated with known alkaloids but structural elucidation revealed it to be **32**, present in the plant primarily as the *N*-oxide. No cryptanthine was observed in the *C. inequata* specimen; alongside known PAs, echiuplateine **33** was identified (as its methyl ester) with comparable abundance ($0.13 \pm 0.001 \text{ mg/g}$ dry weight of plant) to the known echimidine and its *O*-acetyl derivative.

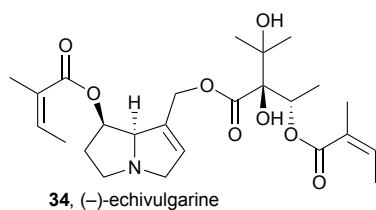


32, (–)-cryptanthine
(* *threo*-isomer proposed)

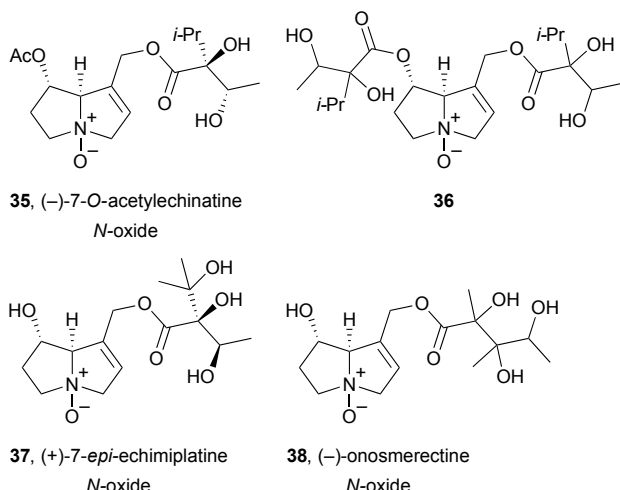


33, echiuplateine
(* undefined)

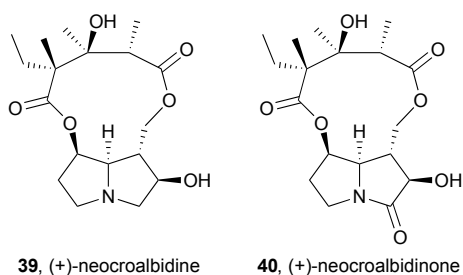
A combination of spectroscopy and computation was used to make a full stereochemical assignment of (–)-echivulgarine **34**, obtained from bee pollen granules presumed to have been collected from *Echium vulgare* (Boraginaceae), commonly occurring in the area.⁴⁹ From 280 g of the granules, 11 mg of the alkaloid were eventually obtained. Full 1H , ^{13}C , and ^{15}N NMR spectra were compared with predicted spectra based on Boltzmann-weighted conformational distributions for candidate stereoisomers. The absolute stereochemical assignment was supported by a comparison of experimental and theoretical circular dichroism (CD) spectra.



The aerial parts of *Onosma erecta* (Boraginaceae) yielded four new pyrrolizidines **35–38**, with structures assigned primarily on the basis of NMR data.⁵⁷ Only limited quantities of **36** and **38** were available and stereochemical assignment of the necic acids was not achieved.

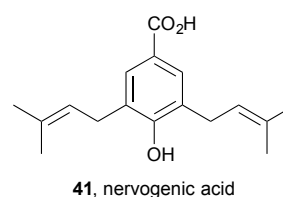


Two new pyrrolizidines, neocroalbidine **39** and neocroalbidinone **40**, were isolated from the herb *Crotalaria albida* (Fabaceae).⁵⁸ Single crystal X-ray diffraction provided structural confirmation of both alkaloids, including their absolute stereochemistry.

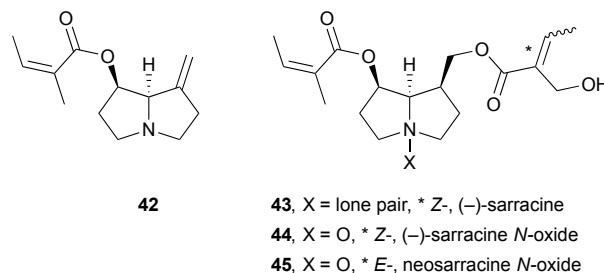


Six new [(+)-nervosines I–VI] and two known [(+)-paludosine, (-)-auriculine] PAs were isolated from *Liparis nervosa* (Orchidaceae).⁵⁹ All are nervogenic acid **41** esters of simple 1-hydroxymethyl pyrrolizidines. Six of these are depicted as esters of (-)-isoretronecanol and two of (-)-trachelanthamidine but the text describes these as esters of their enantiomers, (+)-lindelofidine and (+)-laburnine, respectively. Based on reported structures for the known alkaloids, the structures depicted in the paper show the incorrect enantiomer of the necine base. All eight alkaloids showed no cytotoxicity against human tumour cell lines MCF-7, A549, and HepG2, and most were non-toxic to RAW264.7 macrophages; however, all inhibited lipopolysaccharide- (LPS)

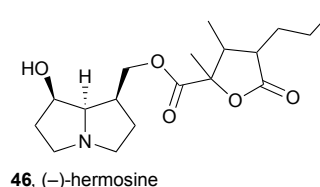
induced NO production in the same cell line with IC₅₀ = 2.16–38.3 μM.



Complete NMR assignments were reported for PAs **42–45** obtained from the roots of *Senecio polypodioides* (Asteraceae), including the novel pyrrolizidine neosarracine N-oxide **45**.⁶⁰

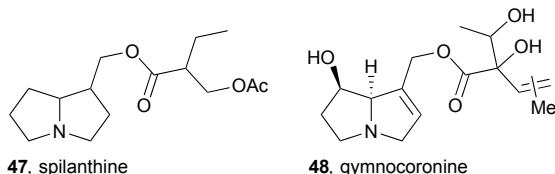


New metabolites were characterised in extracts prepared from transformed root cultures of the plant *Bethencourtia hermosae* (Asteraceae) from La Gomera (Canary Islands).⁶¹ In addition to the known pyrrolizidines senecionine, seneciophylline, and senkirkine, a new pyrrolizidine hermosine **46** was also isolated and characterised through NMR analysis; the stereochemistry around the γ-lactone remained undetermined. Along with many of the other metabolites isolated from this plant, hermosine exhibited some antifeedant activity against aphids.

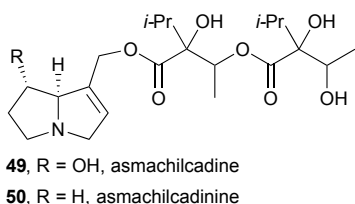


It had been observed that American Monarch butterflies, known to be PA pharmacophagous, are attracted to the freshwater aquatic plant *Gymnocoronis spilanthoides* (Asteraceae) and on this basis Colegate studied the plant's chemical constituents with the expectation that PAs would be found.⁶² Methanol extraction of cultivated whole-plant material and gravimetric analysis of the isolated alkaloidal fractions indicated that approximately 0.08% of the fresh weight of the plant comprised pyrrolizidines. Further HPLC MS/MS analysis revealed at least twenty pyrrolizidines to be present. Along with some known alkaloids (e.g. lycopsamine and intermedine), and a number of unidentified components, two new alkaloids were tentatively identified from MS/MS data as spilanthine **47** and gymnocoronine **48**. This study raised questions on the relative prevalence of toxic PA content in wild vs. cultivated *G. spilanthoides*, implications for human health through potential leaching of these compounds into

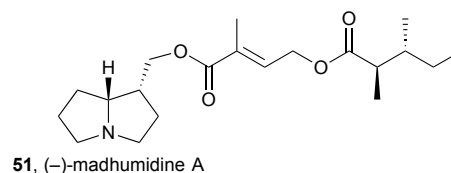
water supplies and the plant's proposed use as a nicotine-free tobacco substitute, and the possibility that this vigorous plant could be used as a sustainable bulk source of PAs.



In a second study guided by the observation of insect attraction to plant material, Colegate's group investigated the components of dried leaves and seed heads of 'asmachilca', a Peruvian botanical medicine derived, in principle but often not in practice, from *Aristeguietia gayana* (Asteraceae) and taken traditionally directly or as a tea, and used as a poultice.⁶³ Again, the study was guided by a concern that toxic pyrrolizidines in these traditional preparations could present a significant chronic threat to human health. Six asmachilca samples were analysed; while there were differences in the HPLC profiles between the samples, and at least two different plant species were present, all contained significant quantities of unsaturated PAs (0.4–0.9 weight/dry weight %). Within the 16 identified pyrrolizidines, two new structures were proposed: asmachilcadine **49**, a heliotridine ester, and asmachilcadinine **50**, the supinidine analogue; the stereochemistry in the necic acids was not confirmed due to inconsistencies with other constituent metabolites present in the extracts. The *N*-oxides were also observed (by MS) in the extracts as confirmed by oxidation of the parents **49** and **50**. Steeping asmachilca samples in boiling water led to alkaloid levels in the tisane that reached a maximum within 3–5 minutes. This work indicates clearly that these preparations present a significant risk of exposure to toxic pyrrolizidines, but variation in the plant source, harvesting, storage, and preparation mean that it is difficult to quantify this risk. Further work is needed to identify the beneficial components of asmachilca preparations with a view to providing a standardised, less toxic preparation.

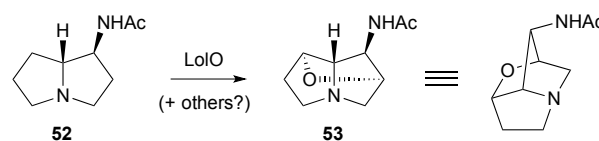


Three lindelofidine [(+)-isotronecanol] esters, one novel, were isolated from the Vietnamese medicinal herb *Madhuca pasquieri* (Sapotaceae).⁶⁴ The structure of the novel pyrrolizidine, (–)-madhumidine **51**, was assigned by NMR experiments; all three alkaloids showed only weak cytotoxicity ($IC_{50} > 100 \mu M$) against three cancer cell lines.



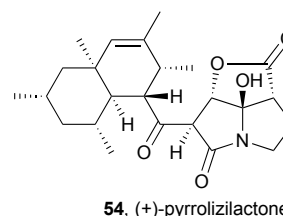
Fungal and bacterial PAs

The lolines, strongly insecticidal secondary metabolites of fungi associated with forage grasses, are distinguished from other pyrrolizidines by an ether linkage connecting C(2) to C(7), as in **53** (Scheme 5). Schardl and co-workers noted accumulation of acetamidopyrrolizidine **52** and no loline production in *lolO*-mutated endophytes.⁶⁵ On this basis the group hypothesised that non-heme iron oxygenase LoIO, possibly in combination with a second enzyme, acts upon biosynthetic intermediate **52** to generate the characteristic loline tricyclic core.

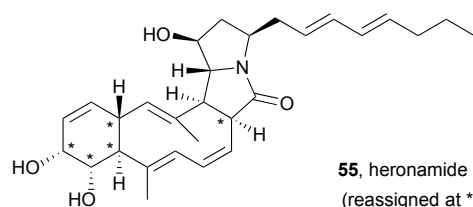


Scheme 5 Biosynthetic incorporation of the C(2)–C(7) ether in the lolines.

Screening of a fungal fraction library led to the isolation and identification of pyrrolizilactone **54**, closely related to cytotoxic antibiotics CJ-16,264 and UCS1025A.⁶⁶ This metabolite was cytotoxic against HL-60 and HeLa cells with $IC_{50} = 1.1$ and $3.1 \mu g mL^{-1}$, respectively, but showed no antibacterial activity (vs. *E. coli* up to $30 \mu g mL^{-1}$).

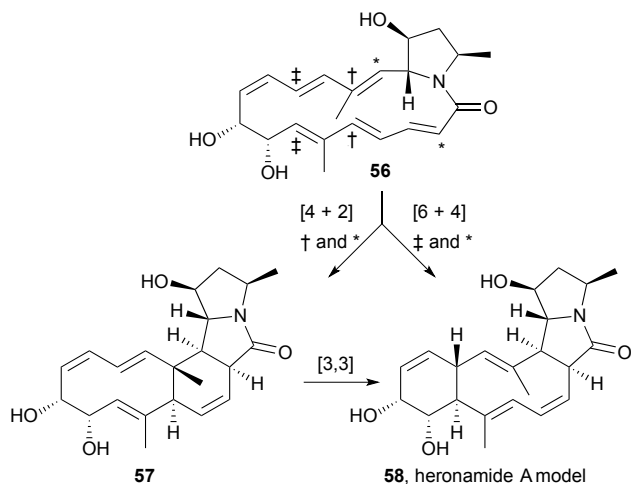


Following a detailed NMR spectroscopic analysis of heronamide A and derivatives, the stereochemistry in this macrocyclic polyketide pyrrolizidinone was reassigned at C(2), C(7–9), and C(12) to that shown (**55**).⁶⁷



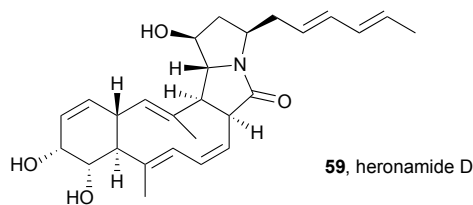
Houk's group reported DFT calculations to support a transannular [6+4] cycloaddition in the formation of heronamide A from heronamide C.⁶⁸ Using a side-chain truncated model **56** (Scheme 6) as the basis for calculations, an ambimodal transition state was located that leads to both the [6+4] adduct **58** and an intermediate intramolecular Diels–

Alder adduct **57** that then undergoes rapid [3,3]-sigmatropic shift (Cope rearrangement) to produce the more stable [6+4] adduct. The results have implications for broader applications of [6+4] cycloadditions in synthesis.



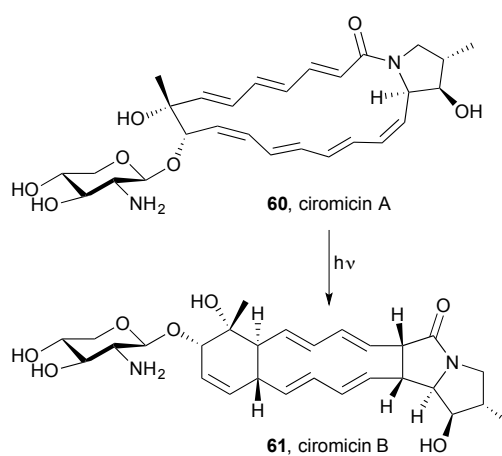
Scheme 6 Parallel one-step and two-step mechanistic pathways connect heronamide A and heronamide C.

Culturing *Streptomyces* sp. SCSIO 03032 in a variety of media resulted in the production and isolation of three new macrolactams, heronamides D–F.⁶⁹ The stereochemistry in heronamide D **59**, assigned by extensive $^3J_{\text{HH}}$ and NOESY NMR spectroscopic analysis, was found to be identical to that in the recently-revised structure for heronamide A (see above); indeed heronamide D differs from heronamide A simply by virtue of a terminal methyl in place of propyl on the dienyl side chain. The three new heronamides showed no antimicrobial activity (against four bacteria and a fungus), no antioxidant activity (DPPH radical scavenging assay), but did exhibit growth inhibition for three of seven cancer cell lines ($\text{IC}_{50} = 15.4\text{--}56.4\ \mu\text{M}$).



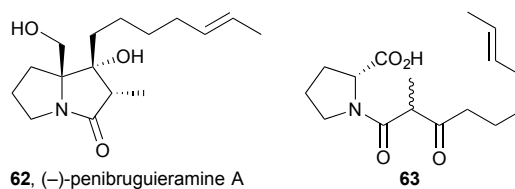
Nocardiopsis sp. FU40 ΔApoS is an engineered bacterium in which the ApoS8 gene, encoding the terminal polyketide synthase, is replaced in order to deactivate the production of apoptolidins. Co-culturing this bacterium with competing bacterial strains activates latent metabolic pathways, leading to the production of secondary metabolites unobserved in monoculture.⁷⁰ A metabolomic response-mapping and comparison approach led to the isolation and identification of a new macrolactam, ciromicin A **60** (Scheme 7), and its isomer ciromicin B **61**, a pyrrolizidinone closely resembling heronamide A **55** and D **59**. The structural elucidation was achieved by a combination of NMR methods once the molecular formula had been established by HRMS. A sample of

pure ciromicin A was converted into ciromicin B, in an overall [6+6] cycloaddition, by exposure to sunlight; ciromicin B was the major product at 400 nm and, although the conversion to ciromicin B reached a maximum at 300 nm, other ciromicin isomers were also produced at this wavelength. The authors propose an outline biosynthesis based on a series of polyketide synthases, then ciromicin-specific enzymes that effect macrolactam formation, closure of the pyrrolidine ring (in ciromicin A), and glycosylation. These new metabolites are structurally and biosynthetically related to cytotoxic macrolactams such as vicenistatin; therefore, their *in vitro* activity was tested against the MV-4-11 human leukaemia cell line and IC_{50} values of 8.1 and 9.3 μM were found for ciromicin A and B, respectively; there was no antibacterial or antifungal activity found in assays with *Bacillus*, *E. coli*, or *Saccharomyces* species.



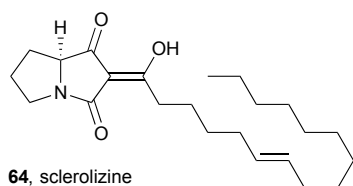
Scheme 7 Ciromicin B is formed by photochemical formal [6+6] cycloaddition within ciromicin A.

The observation of potent antibacterial activity in a crude extract of *Penicillium* sp. strain GD6, isolated from the Chinese mangrove *Bruguiera gymnorrhiza* (Rhizophoraceae), led to the discovery of a new pyrrolizidine, penibrugueramine A **62**.⁷¹ This metabolite is proposed to be biosynthesised from acid **63** which has previously been suggested as a precursor to scalusamide A, a simple fatty acid prolinol amide.

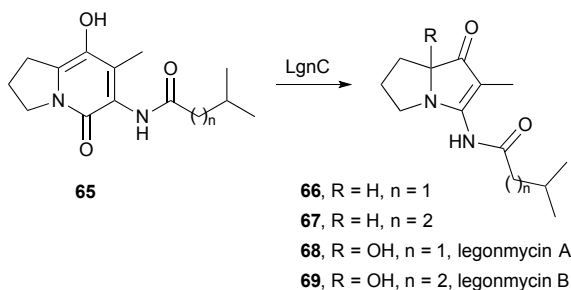


Conceptually related to the induced production of the ciromicins, discussed above, Larsen showed that the growth of the fungus *Aspergillus sclerotiiicarbonarius* in conditions that trigger sclerotium production leads to a greatly altered metabolic profile, with four new compounds identified.⁷² One of these compounds, sclerolizine **64**, is an oxidised pyrrolizidine; the enol stereochemistry was not assigned and the absolute configuration is proposed based solely on a proposed biosynthetic derivation from (*S*)-proline. The four

new metabolites were evaluated as antifungal agents against *Candida albicans*, and sclerolizine was found to be the most potent with $IC_{50} = 8.5 \pm 2.0 \mu M$.



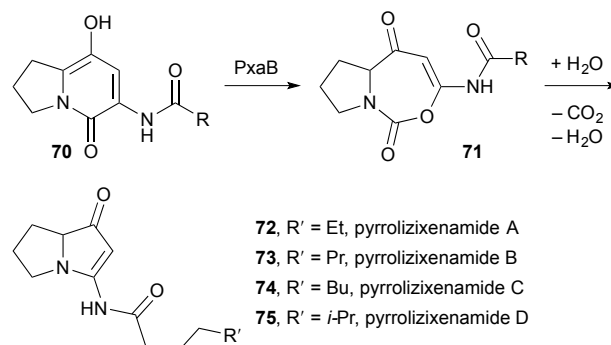
Three papers in quick succession relate to the discovery of bacterial pyrrolizidines of the vinylogous urea type. The first⁷³ reports the isolation, structure, and biosynthesis of legonmycin A **68** and B **69** (Scheme 8), from *Streptomyces* sp. MA37. The structures were elucidated by a combination of spectroscopic and computational techniques and the major metabolite, legonmycin A, obtained as the racemate. From the draft genome for the MA37 strain, the authors were able to identify a gene cluster (*lgn*) encoding four key enzymes: LgnA, a thioesterase; LgnC, a flavin dependent monooxygenase; and LgnB and LgnD, two multidomain non-ribosomal peptide synthetases. A precise role for LgnA was not established but enzymes LgnB and LgnD were shown to assemble legonindolizidine A (**65**, $n = 1$) and B (**65**, $n = 2$). LgnC, along with co-factors FAD^+ , O_2 , and NADPH, then effects a four-step transformation into the legonmycins comprising: (1) a Baeyer–Villiger type oxidative ring-expansion; (2) hydrolysis of the so-formed cyclic carbamate (*cf.* **71** below); (3) decarboxylation then condensation to produce the vinylogous urea functionality (\rightarrow **66** and **67**); then (4) hydroxylation at C(7a).



Scheme 8 The monooxygenase LgnC effects overall decarbonylation and hydroxylation in the biosynthesis of the legonmycins.

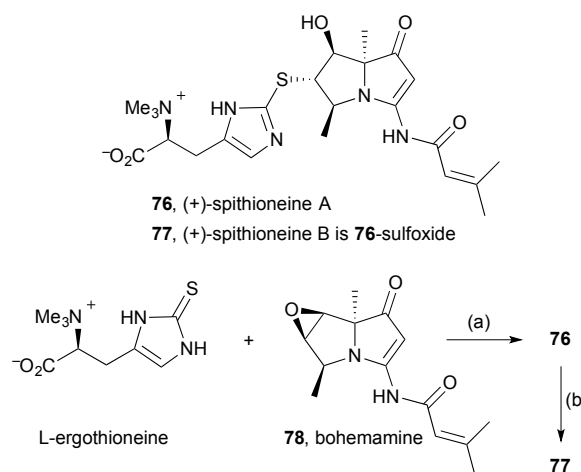
In results that closely parallel those reported by Deng's group in the context of the legonmycins, expression in *E. coli* of an unknown gene cluster from *Xenorhabdus stockiae* and differential analysis by 2D NMR spectroscopy (DANS) led to the isolation and characterisation by NMR and MS methods of pyrrolizixenamides A–C **72–74** (Scheme 9).⁷⁴ The assigned structures were confirmed by total synthesis based on Snider's synthesis of the jenamidines (see previous review). The authors identified a gene cluster *pxaAB* encoding for PxaA, responsible for producing the pyridone intermediates **70** [$R = n$ -pentyl, n -hexyl, n -heptyl], and PxaB that effects a ring-expansion, hydrolysis, and decarboxylative condensation process. The authors also found that more than 90 bacterial strains from 23 species contain *pxaAB* homologues suggesting

that bacterial pyrrolizidines of this type should occur widely. As an example, when the pyrrolizidine gene cluster in *X. szentirmaii* was activated by a promoter exchange method, the branched variant pyrrolizixenamide D **75** was produced.



Scheme 9 Key steps in the biosynthesis of the pyrrolizixenamides.

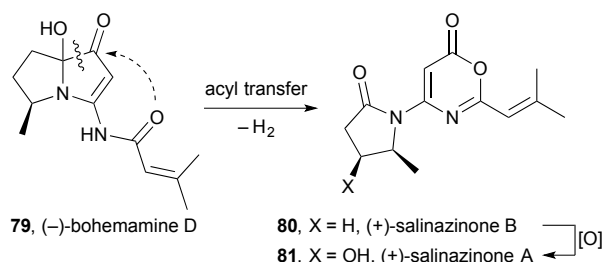
Extracts from the *Streptomyces spinoverrucosus* strain SNB-048 were shown to contain the new pyrrolizidine (+)-spithioneine A **76** and its sulfoxide, spithioneine B **77** (Scheme 10).⁷⁵ In addition to spectroscopic characterisation, the assigned structures were supported by RANEY® Ni desulfurisation (not shown) of spithioneine A that yielded known components bohemiaamine C and (*S*)-hercynine. Additionally, L-ergothioneine and bohemiaamine **78** were combined under basic conditions to achieve a semi-synthesis of spithioneine A, and this was oxidised to give spithioneine B (the sulfoxide stereochemistry was not established). The authors proposed a plausible biosynthesis for these pyrrolizidines initiating with L-ornithine or L-arginine, polyketide extension, then consecutive *N*-cyclisations and dehydrations to give bohemiaamine via bohemiaamine B. The spithioneines were shown to have no cytotoxicity against four lung cancer cell lines and no antibacterial activity against *Pseudomonas aeruginosa* and *Bacillus subtilis*.



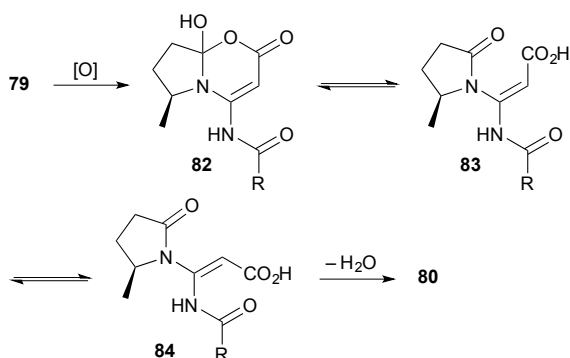
Scheme 10 Reagents and conditions: (a) aq. Na_2CO_3 ; (b) Oxone®, aq. THF, 0 °C.

Two unusual pyrrolidinyloxazinones were isolated from *Streptomyces* sp. KMF-004 extracted from a sea-water salt-making pool in Korea.⁷⁶ Salinazinone B **80** (Scheme 11) and its

hydroxylated counterpart salinazinone **A** **81** were characterised spectroscopically and the absolute configuration assigned by comparison of the experimental and calculated electronic CD spectra. A novel pyrrolizidine, boheminamine **D** **79** and known boheminamine **B** were found in the same bacterial strain and the authors suggest that the salinazinones derive from them biosynthetically. In essence, the authors' mechanism proceeds via C→O acyl transfer (dotted arrow) then oxidation; however, were oxidation to occur first (either on the external nitrogen, the *endo*-double bond or, as shown in Scheme 12, via a Baeyer–Villigerase) then an electronically and sterically more reasonable route arises.



Scheme 11 Originally-proposed order-of-events in the biosynthesis of salinazinone B from boheminamine D.



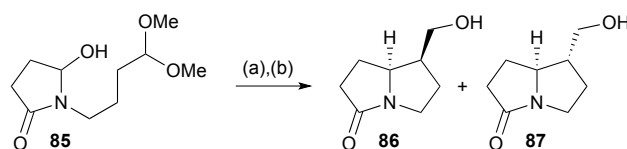
Scheme 12 A hypothesis for the biosynthesis of salinazinone B from boheminamine D.

Synthetic approaches

Isoretronecanol and related molecules⁷⁷

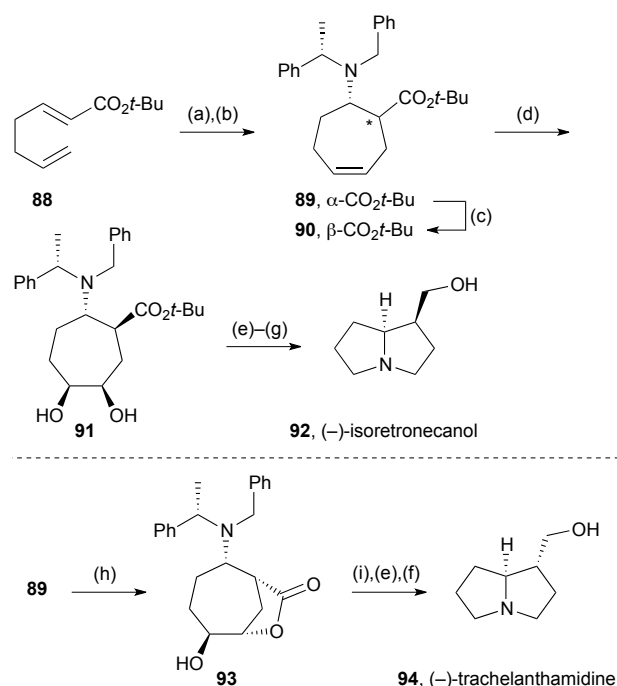
The biosynthetic intramolecular Mannich reaction that introduces the C(1)–C(7a) bond in 1-hydroxymethyl pyrrolizidines inspired a formal synthesis of racemic isoretronecanol (lindelofidine) and trachelanthamidine (laburnine).⁷⁸ The cyclisation of hydroxylactam **85** (Scheme 13), prepared in two steps from succinic anhydride, was evaluated under a range of acid/solvent/temperature combinations to give varying ratios of diastereomers **86** and **87** following reduction of the intermediate aldehyde. Good to high yields were obtained with a full equivalent or more of TsOH. Under most conditions, with acetonitrile as solvent, the *endo*-hydroxymethyl diastereomer **86** predominated (up to 9:1 at 15 °C for 3 h) but this ratio was inverted (1:9) in toluene at 45 °C, presumably reflecting kinetic vs. thermodynamic control, respectively. Lactams **86** and **87** have been converted

previously into (±)-isoretronecanol and (±)-trachelanthamidine, respectively.



Scheme 13 Reagents and conditions: (a) TsOH, CH₃CN, 15 °C or PhCH₃, 45 °C; (b) NaBH₄, MeOH, 0 °C. [86/87 dr = 9:1 (CH₃CN), 1:9 (PhCH₃)]

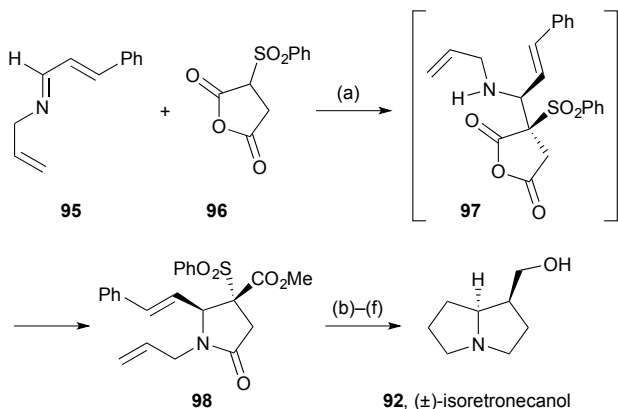
The diene (not shown) formed by diastereoselective 1,4-addition of a chiral ammonia equivalent to enoate **88** (Scheme 14) and enolate allylation *in situ*, was converted into cycloheptylamine derivative **89** by ring-closing metathesis.⁷⁹ The so-formed *cis*-1,2-aminoester was converted efficiently into the *trans*-isomer **90** by reversible enolisation under basic conditions. Alkene dihydroxylation was moderately selective for the face unencumbered by the amino substituent (dr = 80:20) but this was of no consequence since the next step cleaved this diol (**91**) to generate a dialdehyde. After amine deprotection, double reductive amination and ester reduction provided (–)-isoretronecanol **92**. Alternatively, alkene epoxidation in diastereomeric substrate **89** gave hydroxylactone **93**, with the initial epoxidation stereochemistry presumed to result from steric control. Reductive lactone cleavage followed by a parallel end-sequence to that used for (–)-isoretronecanol afforded (–)-trachelanthamidine **94**. A variant of each route was also applied to the opposite ester **89/90** diastereomer to provide a second synthesis of both alkaloids.



Scheme 14 Reagents and conditions: (a) lithium (*S*)-*N*-benzyl-*N*-(α-methylbenzyl)amide, THF, –78 °C then allyl bromide; (b) Grubbs I, CH₂Cl₂, 30 °C; (c) KHMDS, *t*-BuOH, THF; (d) OsO₄, TMEDA, CH₂Cl₂, –78 °C then P(CH₂OH)₃, Et₃N, SiO₂; (e) NaIO₄, MeOH; (f) H₂, Pd/C, MeOH; (g) NaBH₄, MeOH; (h) NaBH₄, MeOH.

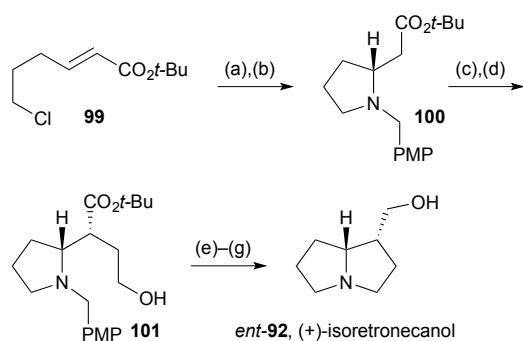
$\text{Pd}(\text{OH})_2/\text{C}$, AcOH, MeOH; (g) DIBAL, THF, 0 °C; (h) HBF_4 , MCPBA, CH_2Cl_2 ; (i) LiAlH_4 , THF, 0 °C.

Methodology developed for the stereoselective synthesis of γ - and δ -lactams was applied to (\pm)-isoretronecanol (lindelofidine).⁸⁰ Proton transfer from sulfonyl anhydride **96** (Scheme 15) to imine **95**, followed by Mannich-type addition, gave intermediate **97** with excellent diastereoselectivity ($dr > 95:5$). *O*- to *N*-acyl transfer proceeded under the reaction conditions and esterification *in situ* gave lactam **98**. The second ring was introduced by ring-closing metathesis, and reductive steps completed the route.



Scheme 15 Reagents and conditions: (a) THF then $\text{Me}_3\text{SiCHN}_2$, MeOH, PhCH_3 , 0 °C; (b) Grubbs II, C_6H_6 , reflux; (c) H_2 , Pd/C, MeOH; (d) DBU, CHCl_3 ; (e) H_2 , Pd/C, MeOH; (f) LiAlH_4 .

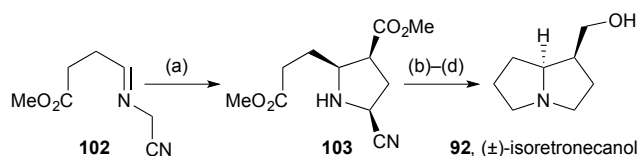
Davies' group described a synthesis of the (+)-enantiomer of isoretronecanol (that is, lindelofidine), along with indolizidine and quinolizidine analogues, again based on their chiral ammonia methodology.⁸¹ 1,4-Addition of the lithiated chiral amine (step a, Scheme 16) to enoate **99** gave the adduct as a single diastereomer. This was not isolated but subjected to immediate Finkelstein reaction; the so-formed iodide cyclised under the reaction conditions with loss of the *N*- α -methyl-PMB group providing pyrrolidine **100** in 63% overall yield from **99**. Ester enolate alkylation with a protected 2-hydroxyethyl electrophile proceeded with high diastereoselectivity, in accordance with the group's previous work, and from **101** completion of the synthesis required just three straightforward steps.



Scheme 16 Reagents and conditions: (a) lithium (*R*)-*N*-*p*-methoxybenzyl-*N*-(α -methyl-*p*-methoxybenzyl)amide, THF, -78 °C; (b) NaI, CH_3CN , reflux; (c) LiHMDS, THF, -78 °C then

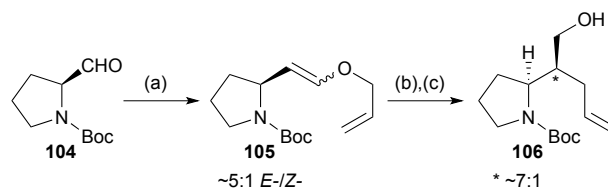
$\text{TBSO}(\text{CH}_2)_2\text{I}$, -78 °C \rightarrow rt; (d) PPTS, MeOH, CH_2Cl_2 , 50 °C; (e) I_2 , polymer-supported PPh_3 , CH_3CN , PhCH_3 ; (f) H_2 , $\text{Pd}(\text{OH})_2/\text{C}$, MeOH; (g) LiAlH_4 , THF, reflux.

General methodology for the synthesis of 2,3-*cis*-disubstituted pyrrolidines was applied to the synthesis of racemic isoretronecanol.⁸² Ag(I)-catalysed azomethine ylid cycloaddition of iminonitrile **102** (Scheme 17) with methyl acrylate gave 2-cyanopyrrolidine **103** as the single *endo*-diastereomer shown. A novel procedure for reductive decyanation was developed that the authors proposed to proceed via borohydride mediated E2-type elimination of HCN and then reduction of the so-formed borane-complexed pyrroline with NaBH_3CN generated *in situ*. The route was completed by lactamisation and reduction of both carbonyl groups.



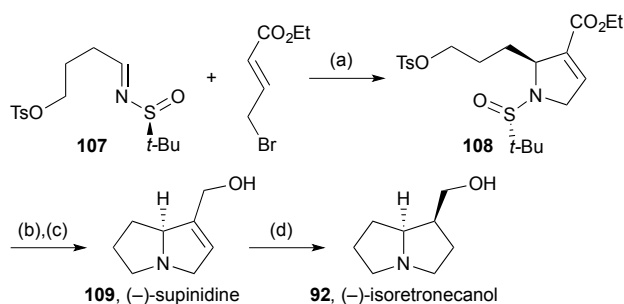
Scheme 17 Reagents and conditions: (a) methyl acrylate, AgOAc, DBU, PhCH_3 , 0 °C; (b) NaBH_4 , $\text{BH}_3\cdot\text{THF}$, THF; (c) PhCH_3 , reflux; (d) LiAlH_4 , THF, reflux.

Gavhane achieved a formal synthesis of (–)-isoretronecanol and (–)-trachelanthamidine based on Claisen rearrangement.⁸³ Wittig reaction of *N*-Boc-(*S*)-prolinal **104** (Scheme 18) gave a mixture of diastereomers **105**. These diastereomers were taken on into the thermal rearrangement step and a 7:1 ratio of aldehyde epimers (not shown) was obtained. The authors made no comment on the origin of this preferred stereochemistry nor its relation to the ~5:1 *E*-/*Z*-ratio of enol ether diastereomers. Reduction to alcohol **106** and its epimer completed a formal synthesis that connects with Knight's 1997 route that employed a related, but poorly-stereoselective Ireland–Claisen rearrangement ($dr = 1\text{--}2:1$) as the key step.⁸⁴



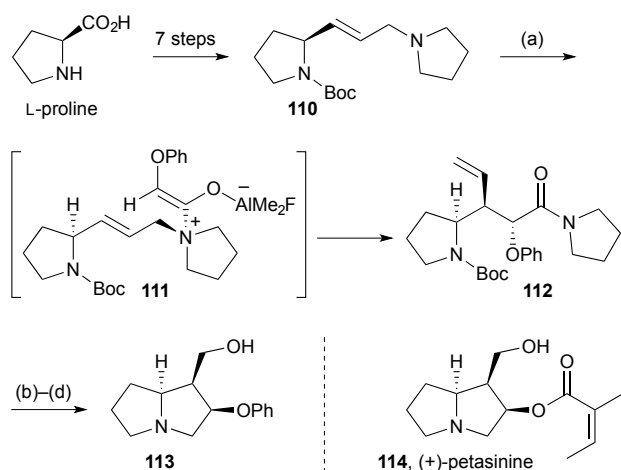
Scheme 18 Reagents and conditions: (a) $\text{Ph}_3\text{P}^+\text{CH}_2\text{OCH}_2\text{CH}=\text{CH}_2$, *t*-BuOK, PhCH_3 , 0 °C; (b) C_6H_6 , 80 °C; (c) NaBH_4 , MeOH, 0 °C.

Njardarson reported⁸⁵ an asymmetric variant of methodology for 2-arylpyrroline synthesis originally described by Steel.⁸⁶ In one application, addition of the dienolate derived from ethyl bromocrotonate to chiral sulfinylimine **107** (Scheme 19) afforded the (2*S*)-alkylpyrroline **108** as a single diastereomer. Acidic hydrolysis of the *N*-sulfinyl group and cyclisation of the resulting free amine completed the pyrrolizidine core. Reduction of the ester gave (–)-supinidine **109**, six steps overall from butane-1,4-diol and the shortest asymmetric synthesis of this alkaloid; *exo*-face hydrogenation of the alkene gave (–)-isoretronecanol **92**.



Scheme 19 Reagents and conditions: (a) LDA, THF, -78°C ; (b) TMSCl, aq. MeOH then Et_3N , CH_2Cl_2 ; (c) DIBAL, CH_2Cl_2 , 0°C ; (d) H_2 , Pd/C, CH_2Cl_2 .

Access to the necine base core of (+)-petasine **114** (Scheme 20), petasinecine [(2*R*)-hydroxy-(−)-isoretronecanol], was achieved in an enantiospecific route from (*S*)-proline.⁸⁷ The key step in the sequence, aza-Claisen rearrangement of ketene adduct **111**, gave amide **112** as a single stereoisomer. Boc deprotection, lactamisation, and ozonolysis of the vinyl side chain gave *O*-phenyl petasinecine **113**.

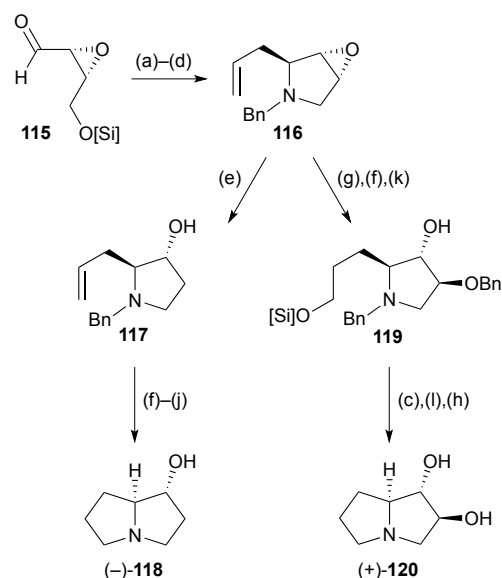


Scheme 20 Reagents and conditions: (a) α -phenoxyacetyl fluoride, AlMe_3 , Na_2CO_3 , CH_2Cl_2 , $0^{\circ}\text{C} \rightarrow \text{rt}$; (b) SOCl_2 , MeOH, reflux; (c) O_3 , MeOH, -78°C then NaBH_4 , MeOH, -78°C ; (d) $\text{BH}_3\text{-SMe}_2$, THF, $0^{\circ}\text{C} \rightarrow \text{rt}$.

Simple hydroxypyrrolizidines

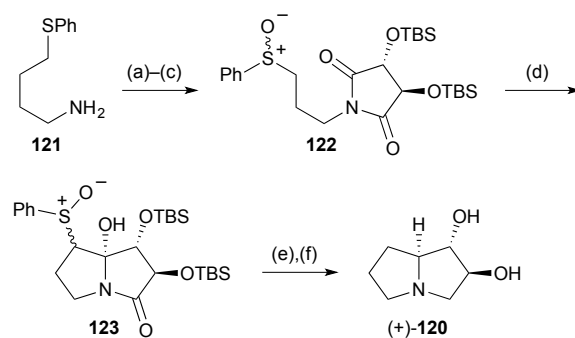
The epoxyaldehyde (*R,R*)-**115** (Scheme 21), derived in three steps from *cis*-but-2-en-1,4-diol, was the starting point for enantioselective syntheses of (1*R*,7*aS*)-1-hydroxypyrrolizidine **118** and (1*S*,2*S*,7*aS*)-1,2-dihydroxypyrrolizidine **120**.⁸⁸ The 1,7*a*-relative stereochemistry in both pyrrolizidines was established by diastereoselective allylation of the benzylimine derived from aldehyde **115**; cyclisation then followed under standard Appel halogenation conditions. From intermediate **116**, the routes diverged, with epoxide reduction (step e) leading, ultimately, to the monohydroxylated product **118**. The *trans*-diol motif in **120** was established by Lewis acid mediated epoxide alcoholysis (\rightarrow **119**), with straightforward deprotection and cyclisation steps completing the route. In both routes, regioselective epoxide-opening may be considered to proceed via $\text{S}_{\text{N}}2$ -like delivery of hydride or benzyl alcohol at the less sterically encumbered 4-position,

which also results in the least reorganisation of the pyrrolidine ring conformation.



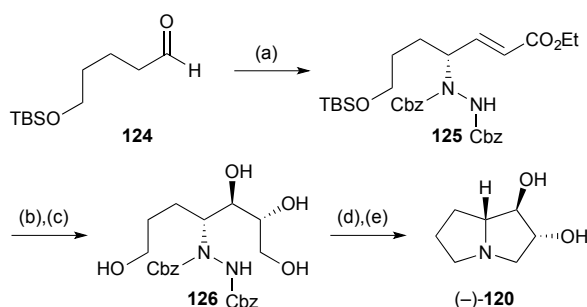
Scheme 21 Reagents and conditions: (a) BnNH_2 , Et_2O ; (b) $\text{CH}_2=\text{CHCH}_2\text{MgBr}$, $\text{BF}_3\cdot\text{OEt}_2$, Et_2O , -78°C ; (c) $\text{NH}_4\text{F}\cdot\text{HF}$, MeOH; (d) PPh_3 , CCl_4 , Et_3N , DMF; (e) LiAlH_4 , Et_2O ; (f) TBPSCl, imidazole, DMF; (g) 9-BBN, THF then NaOH, aq. H_2O_2 ; (h) $\text{NH}_4^+\text{HCO}_2^-$, Pd/C, MeOH, reflux; (i) PPh_3 , CCl_4 , Et_3N , DMF; (j) TBAF, THF; (k) BnOH , $\text{Yb}(\text{OTf})_3$, dioxane, 80°C ; (l) TsCl , pyridine, CH_2Cl_2 .

Two further syntheses of the lower homologue of lentiginosine, (1*S**,2*S**,7*aS**)-dihydroxypyrrolizidine **120**, were reported during the review period. The first, of the (+)-enantiomer (Scheme 22), began with imide formation from L-(+)-tartaric acid, *O*-silylation, and sulfide oxidation to give tartarimide derivative **122**.⁸⁹ α -Sulfinyl anion addition *anti*-to the adjacent TBSO-substituent afforded a mixture of inseparable C(7)- and S-stereoisomers **123**. Following reductive cleavage of the sulfinyl group, treatment with LiAlH_4 achieved stereoselective reduction of the C(7*a*)-hydroxy group, reduction of the lactam, and desilylation of the hydroxy groups. The stereoselectivity of the reduction at C(7*a*) was proposed to arise from pseudoaxial delivery of hydride to the *N*-acyl iminium in a conformation with pseudoequatorial TBSO-substituents in the pyrrolidine ring.



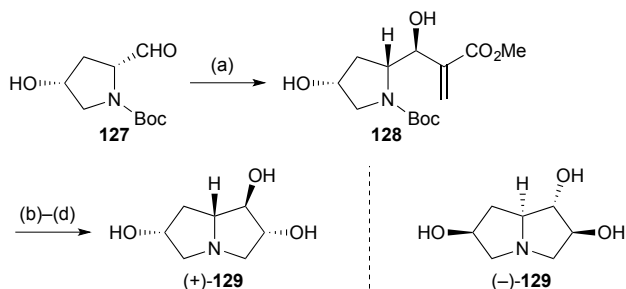
Scheme 22 Reagents and conditions: (a) L-(+)-tartaric acid, xylene, reflux; (b) TBSCl, imidazole, DMF, $0^{\circ}\text{C} \rightarrow \text{rt}$; (c) NaIO_4 , aq. MeOH, $0^{\circ}\text{C} \rightarrow \text{rt}$; (d) LiHMDS , THF, -78°C ; (e) $\text{NiCl}_2\cdot 6\text{H}_2\text{O}$, NaBH_4 , aq. MeOH; (f) LiAlH_4 , THF, reflux.

Kumar's synthesis of the (–)-enantiomer (Scheme 23)⁹⁰ was elaborated from the hydrazide (not shown) formed by organocatalytic amination of aldehyde **124**. Enoate **125** was obtained with '94% enantioselectivity' after HWE olefination *in situ* using Masamune–Roush conditions. The final stereocentres were then introduced by Sharpless asymmetric dihydroxylation although there is some disparity between the synthetic scheme in the paper, where (DHQD)₂PHAL is cited as ligand system, and the text which refers to (DHQD)₂AQN. Regardless, the relative stereochemical outcome in this step (dr = 25:75 in favour of that shown in **126**) is counter to the inherent 83:17 ratio (in favour of the *syn,syn*-isomer) obtained for a homologue of **125**. Sulfonylation of the 1°-hydroxyls, and hydrogenolysis to reveal the free amine, led to double cyclisation to complete the synthesis.



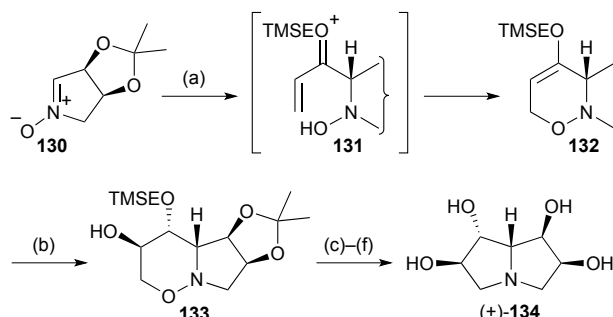
Scheme 23 Reagents and conditions: (a) dibenzyl azodicarboxylate, (*S*)-proline (8 mol%), CH₃CN, 0 °C → 10 °C then add LiCl, (EtO)₂POCH₂CO₂Et, DBU, 5 °C; (b) OsO₄, K₃Fe(CN)₆, K₂CO₃, (DHQD)₂AQN, MsNH₂, aq. *t*-BuOH, 0 °C; (c) LiBH₄, THF, 0 °C; (d) TsCl, Et₃N, CH₂Cl₂, 0 °C → rt; (e) H₂, RANEY® Ni, MeOH then EtOH, 55 °C.

Both enantiomers of a 6-hydroxy derivative of the lentiginosine homologues described above were prepared in short sequences from commercially available 4-hydroxyproline.⁹¹ Thus, 4-hydroxyprolinal **127** (Scheme 24) was prepared in three steps from the (*R,R*)-enantiomer and subjected to Morita–Baylis–Hillman addition of methyl acrylate. The almost complete stereoselectivity in this reaction (step a) was explained by a Felkin–Anh approach to the aldehyde in a conformation stabilised by H-bonding to the hydroxy group. Release of the free amino group, lactamisation, and ozonolysis with a reductive work-up gave the *trans*-1,2-diol stereochemistry present in the final product (+)-**129**. Lactam reduction completed the route and the sequence was repeated from (4*S*)-hydroxy-(*S*)-proline to give (–)-**129**.



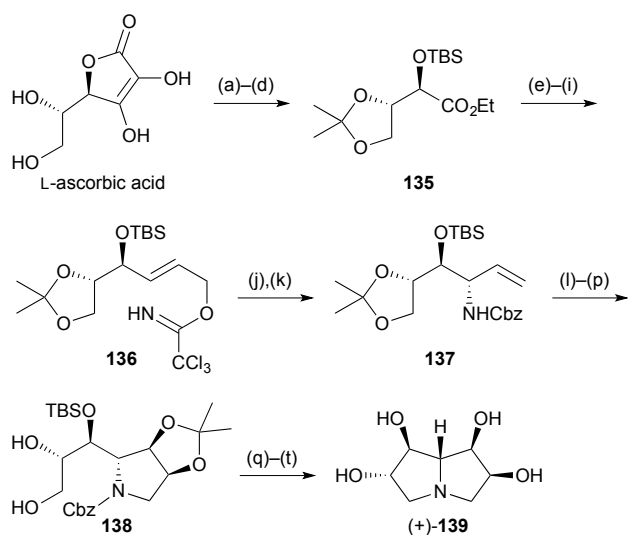
Scheme 24 Reagents and conditions: (a) methyl acrylate, DABCO, sonication; (b) aq. HCl, PhCH₃, 0 °C then aq. NaOH, 0 °C; (c) O₃, MeOH, CH₂Cl₂, –78 °C then NaBH₄, –78 °C → rt; (d) LiAlH₄, AlCl₃, THF, reflux.

Two syntheses of simple tetrahydroxy pyrrolizidines have been described during the review period, the first being an enantiospecific route from L-erythrose.⁹² α-Lithio-1-[2-(trimethylsilyl)ethoxy]allene added to the *exo*-face of nitron **130** (Scheme 25) then (presumably) acid-catalysed 6-*endo-trig* *O*-cyclisation followed *via* intermediate **131**. The resulting cyclic enol ether **132** was hydroborated on the less hindered face and oxidised to afford alcohol **133** with all stereocentres set. Formation of the pyrrolizidine ring system was achieved by protection of the free hydroxy group, N–O reduction with Sm(II), then *N*-cyclisation *via* the mesylate. The final product **134** had been shown previously to be an inhibitor of amyloglucosidase from *Rhizopus* sp.



Scheme 25 Reagents and conditions: (a) 2-[(trimethylsilyl)ethoxy]allene, BuLi, THF, –78 °C then MgSO₄; (b) BH₃·THF, THF, –30 °C → rt then aq. NaOH, H₂O₂, –10 °C → rt; (c) TBDPSCI, imidazole, DMAP, CH₂Cl₂, 0 °C → rt; (d) SmI₂, THF; (e) MsCl, pyridine, 0 °C → rt; (f) Dowex-50, EtOH, 65 °C.

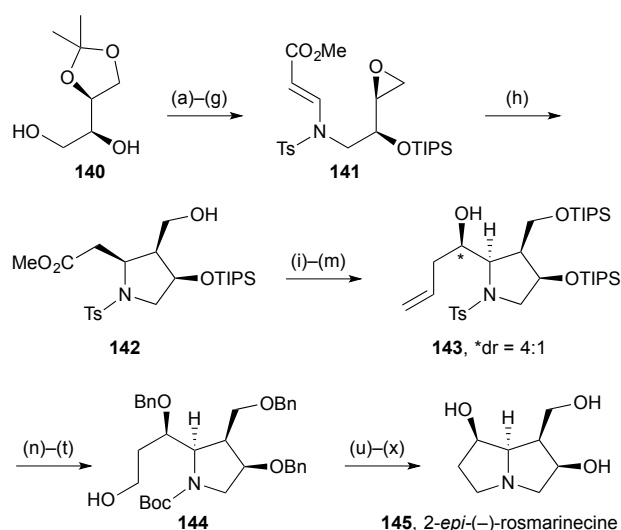
In the second synthesis, the 6,7-di-*epi*-diastereomer of pyrrolizidine **134** was prepared in ~20 steps from L-ascorbic acid (Scheme 26).⁹³ Allylic trichloroacetimidate **136** was prepared by routine redox transformations and protecting group steps. This, the corresponding *O*-benzyl ether, and the free alcohol were studied as substrates for both thermal and Pd(II)-catalysed Overman rearrangement to establish the 7a-stereogenic centre. Among these, only the TBS derivative **136** gave a single 7a-diastereomer and the yield was much improved in the Lewis acid catalysed reaction at room temperature (81%) compared with heating at reflux in xylene (23%). From allylic amine **137** the first ring was constructed by RCM then, after dihydroxylation and acetonide protection, the pyrrolizidine was completed by regioselective *O*-sulfonylation then global deprotection. Purification via the tetracetate gave the target pyrrolizidine with data in accordance with those obtained by Robina's group as described in the previous review.



Scheme 26 Reagents and conditions: (a) CuSO_4 , acetone; (b) aq. H_2O_2 , K_2CO_3 ; (c) EtI , CH_3CN , reflux; (d) TBSCl , imidazole, DMF ; (e) DIBAL , CH_2Cl_2 , -10°C ; (f) IBX , DMSO ; (g) $\text{Ph}_3\text{P}=\text{CHCO}_2\text{Et}$, CH_2Cl_2 , reflux; (h) DIBAL , CH_2Cl_2 , -30°C ; (i) Cl_3CCN , DBU , 0°C ; (j) $\text{PdCl}_2(\text{CH}_3\text{CN})_2$, *p*-benzoquinone, PhCH_3 ; (k) NaOH , aq. THF , 65°C then CbzCl , RT ; (l) NaH , allyl bromide, TBAI , DMF ; (m) Grubbs I, CH_2Cl_2 ; (n) OsO_4 , NMO , *t*-BuOH, aq. acetone; (o) $\text{Me}_2\text{C}(\text{OMe})_2$, TsOH , CH_2Cl_2 ; (p) $\text{Zn}(\text{NO}_3)_2 \cdot 6\text{H}_2\text{O}$, CH_3CN , 50°C ; (q) Bu_2SnO , TsCl , Et_3N , CH_2Cl_2 ; (r) H_2 , $\text{Pd}(\text{OH})_2/\text{C}$, MeOH then aq. HCl ; (s) Ac_2O , pyridine; (t) aq. NH_3 , MeOH .

Rosmarinacines

Chakraborty's synthesis of 2-*epi*-(–)-rosmarininecine **145** (Scheme 27) featured Nugent–Rajanbabu–Gansäuer epoxide reductive radical cyclisation of vinylogous carbamate **141**.⁹⁴ This reaction gave trisubstituted pyrrolidine **142** apparently as a single diastereomer. The authors rationalise the outcome as resulting from a Beckwith–Houk transition state assembly with a pseudoaxial (bulky) silyloxy substituent. The C(7)-hydroxy group stereochemistry was set by diastereoselective allylation with allyltributylstannane and Lewis acid activation of the aldehyde (step m); no diastereoselectivity was observed using allylmagnesium bromide. Despite the efficient construction of the first ring (step h), the overall route is long (~27 steps from L-ascorbic acid), in part due to the >10 protecting group manipulations throughout the synthesis.

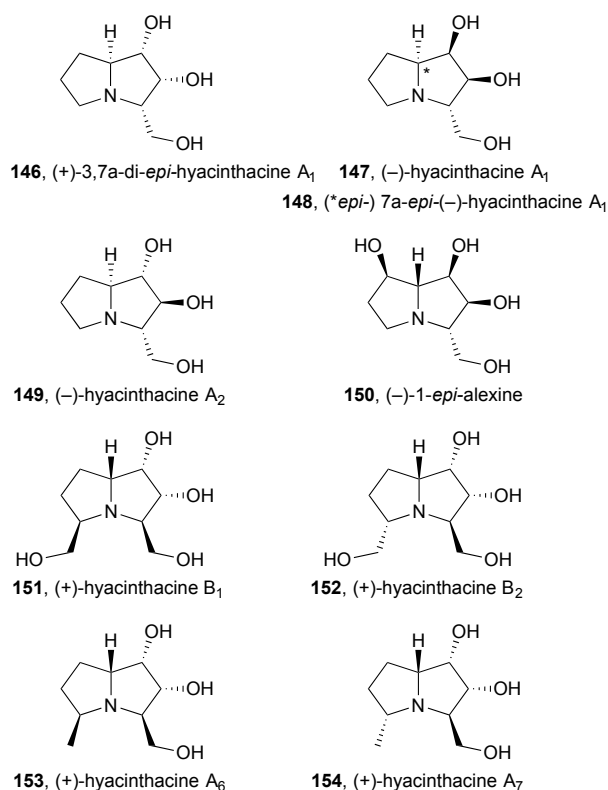


Scheme 27 Reagents and conditions: (a) Bu_2SnO , Et_3N , TsCl , CH_2Cl_2 , 0°C ; (b) TIPSOTf , Et_3N , CH_2Cl_2 , 0°C ; (c) TsNH_2 , KOH , DMSO , 80°C ; (d) methyl propiolate, NMM , CH_2Cl_2 ; (e) aq. AcOH , 100°C ; (f) Bu_2SnO , Et_3N , TsCl , CH_2Cl_2 , $0^\circ\text{C} \rightarrow \text{rt}$; (g) NaH , DMF , 0°C ; (h) Cp_2TiCl_2 , Zn , ZnCl_2 , THF , $-20^\circ\text{C} \rightarrow \text{rt}$; (i) TIPSOTf , Et_3N , CH_2Cl_2 , 0°C ; (j) DIBAL , CH_2Cl_2 , $-78^\circ\text{C} \rightarrow 0^\circ\text{C}$; (k) TBSCl , DBU , CH_2Cl_2 ; (l) O_3 , pyridine, MeOH , CH_2Cl_2 , -78°C then PPh_3 ; (m) allyl-SnBu₃, $\text{BF}_3 \cdot \text{OEt}_2$, CH_2Cl_2 , -78°C ; (n) Na , naphthalene, THF , -78°C ; (o) Boc_2O , Et_3N , CH_2Cl_2 ; (p) TBAF , THF ; (q) BnBr , $\text{Bu}_4\text{N}^+\text{F}^-$, DMF , THF ; (r) OsO_4 , NMO , PhCH_3 , aq. acetone; (s) NaIO_4 , aq. THF , 0°C ; (t) NaBH_4 , MeOH , 0°C ; (u) TsCl , Et_3N , DMAP , CH_2Cl_2 ; (v) TFA , CH_2Cl_2 , 0°C ; (w) K_2CO_3 , EtOH , reflux; (x) H_2 , $\text{Pd}(\text{OH})_2$, MeOH .

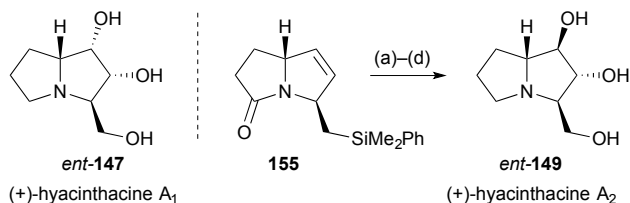
Hyacinthacines and their analogues

The more heavily hydroxylated PAs, notably the hyacinthacines, casuarines, and australines, continue to attract attention as targets to highlight stereoselective synthetic methodology and, in combination with their analogues, for biological screening, especially as glycosidase inhibitors.

D-Ribose was used as starting material for a formal synthesis of (+)-3,7a-di-*epi*-hyacinthacine **A₁ 146** [= (+)-2-*epi*-hyacinthacine **A₂**].⁹⁵ Davies provided full details⁹⁶ of syntheses of (–)-hyacinthacine **A₁**, (–)-7a-*epi*-hyacinthacine **A₁**, (–)-hyacinthacine **A₂**, and (–)-1-*epi*-alexine **147–150** that were covered in the previous review. Delair and Greene applied their approach from Stericol® as a chiral auxiliary, as reviewed previously, to (+)-hyacinthacine **B₁ 151** and (+)-hyacinthacine **B₂ 152**⁹⁷ and, later, to (+)-hyacinthacine **A₆ 153** and (+)-hyacinthacine **A₇ 154**.⁹⁸

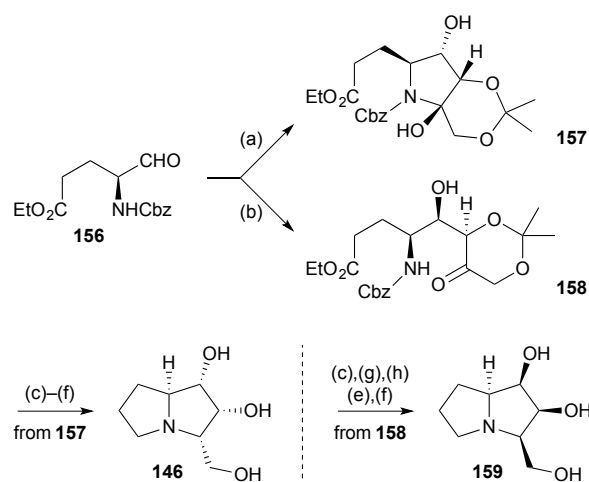


Subsequently, the group reported the synthesis of (+)-hyacinthacine A₂ *ent*-**149** (Scheme 28).⁹⁹ Pyrrolizidinone **155**, that was an intermediate for the synthesis of (+)-hyacinthacine A₁ *ent*-**147** (summarised in the previous review), was epoxidised and hydrolysed to give the 1,2-*trans*-diol functionality. Fleming–Tamao oxidation of the silyl substituent and lactam reduction completed the route.



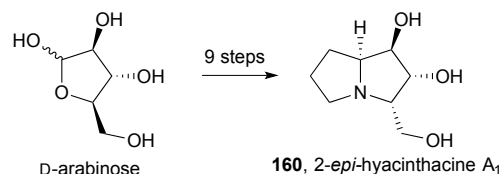
Scheme 28 Reagents and conditions: (a) CF₃COCH₃, Oxone®, EDTA, Na₂CO₃, CH₃CN; (b) CF₃CO₂H, aq. THF, 70 °C; (c) HBF₄·OMe₂, CH₂Cl₂ then KF, MCPBA, DMF; (d) BH₃·SMe₂, THF.

Concise syntheses of (+)-2-*epi*-hyacinthacine A₂ **146** and (–)-3-*epi*-hyacinthacine A₁ **159** (Scheme 29) were achieved from (*S*)-glutamic acid *via* aldehyde **156**.¹⁰⁰ Reagent controlled organocatalytic aldol addition of 2,2-dimethyl-1,3-dioxan-5-one to this aldehyde with the (*S*)- and (*R*)-enantiomers of the proline catalyst resulted in diastereomers **157** and **158**, respectively, the former existing predominantly in the hemiaminal form shown. These two intermediates were then taken separately through short sequences of deprotection and reductive amination to provide the target molecules.



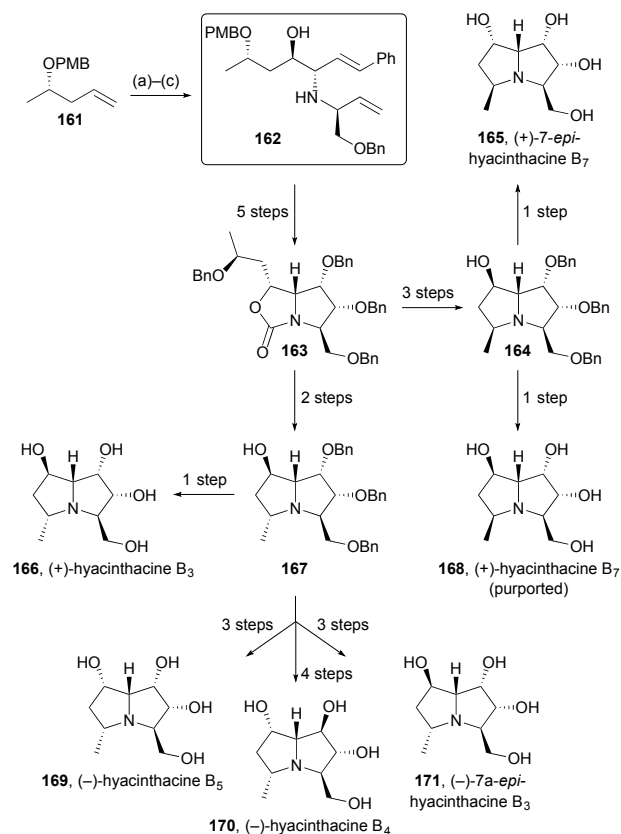
Scheme 29 Reagents and conditions: (a) 2,2-dimethyl-1,3-dioxan-5-one, (*S*)-proline, DMF [dr = 6:1]; (b) 2,2-dimethyl-1,3-dioxan-5-one, (*R*)-proline, DMF [dr = 10:1]; (c) H₂, Pd/C, EtOH; (d) K₂CO₃, EtOH; (e) LiAlH₄, THF, reflux; (f) aq. HCl, MeOH; (g) TBSOTf, 2,6-lutidine, CH₂Cl₂, 0 °C; (h) TBAF, THF.

A synthesis of 2-*epi*-hyacinthacine A₁ **160** (Scheme 30) was achieved from D-arabinose with the C(5)–C(7) carbons being introduced by iminium allylation and subsequent hydroboration.¹⁰¹



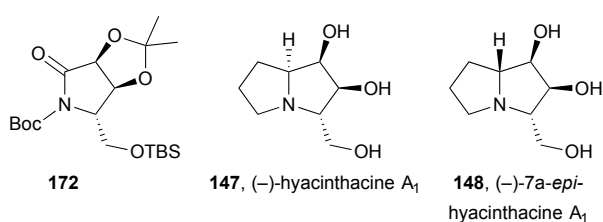
Scheme 30 Enantiospecific synthesis of 2-*epi*-hyacinthacine A₁.

Pyne described an improved method for the preparation of key intermediate **162** (Scheme 31) that has been used for the synthesis of several pyrrolizidines. The new route dispensed with the need for a vinyl sulfone starting material by switching from (DHQD)₂PHAL to (DHQD)₂PYR as ligand system for the dihydroxylation reaction (step a).¹⁰² This intermediate was then employed in the synthesis of six hyacinthacine isomers using routes analogous to those detailed in the previous review. The authors concluded that the structures of hyacinthacines B₃ **166**, B₄ **170**, and B₅ **169** are correctly reported in the earlier literature but hyacinthacine B₇ **168** is incorrectly assigned; they further suggest that natural hyacinthacines B₅ and B₇ are the same compound, although this proposal could not be proven.



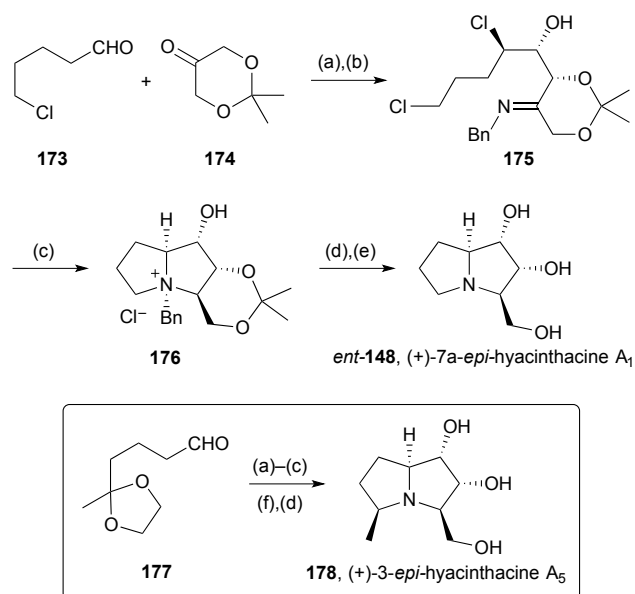
Scheme 31 Reagents and conditions: (a) K_2OsO_4 , $K_3Fe(CN)_6$, $MsNH_2$, $(DHQD)_2Pyr$, aq. t -BuOH; (b) TEMPO, NaOCl, aq. $NaHCO_3$, CH_2Cl_2 ; (c) styryl boronic acid, (S)-1-(benzyloxy)but-3-en-2-amine, CH_2Cl_2 .

(-)-Hyacinthacine **A₁** **147** and its 7a-epimer **148** were prepared from lactam **172** obtained from D-glutamic acid.¹⁰³ Allyl addition to an iminium ion at pro-C(7a) set the stereochemistry for 7a-*epi*-hyacinthacine **A₁**. For hyacinthacine **A₁** itself, lactam **172** was allylated directly giving a ketone which was then reduced and the desired alcohol cyclised *via* the mesylate.



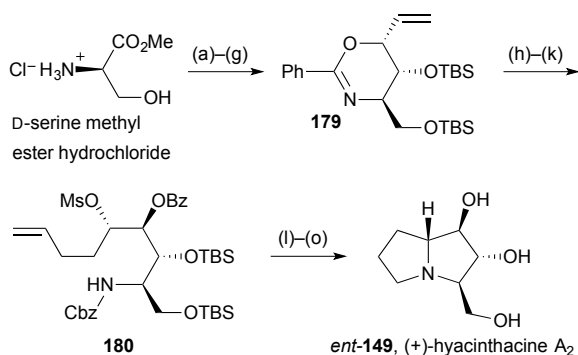
Britton reported a general approach to the asymmetric synthesis of iminosugars based on tandem proline-catalysed α -chlorination then aldol reaction with dihydroxyacetone derivative **174** to establish a 2,3-dihydroxy-4-chlorocarbonyl stereotriad.¹⁰⁴ Two pyrrolizidines were prepared in short routes (Scheme 32). The first, from aldehyde **173**, gave ammonium salt **176** in ~98% ee, via imine **175**. Hydrogenolysis and acetonide hydrolysis completed the five step route to (+)-7a-*epi*-hyacinthacine **A₁** with 43% overall yield. Alternatively, starting with protected ketoaldehyde **177** and effecting the second cyclisation by reductive amination, (+)-3-*epi*-

hyacinthacine **A₅** was obtained in 35% overall yield, again with ~98% ee.



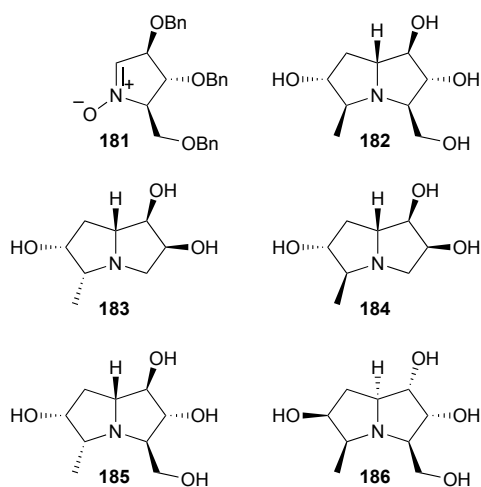
Scheme 32 Reagents and conditions: (a) NCS, (S)-proline, CH_2Cl_2 ; (b) $BnNH_2$, AcOH, 4 Å MS, THF then $NaBH_3CN$; (c) $NaHCO_3$, $PhCH_3$, 105 °C; (d) H_2 , MeOH, 60 °C (H-Cube) [then for **178** Dowex 1X8-100 (HO^- form)]; (e) $NaHCO_3$, MeOH, 80 °C then PPTS, aq. MeOH, 100 °C then Dowex 1X8-100 (HO^- form); (f) PPTS, aq. MeOH, 100 °C.

An enantiospecific synthesis of (+)-hyacinthacine **A₂** began with *N*- and *O*-protection of D-serine then addition of a 2-(chloromethyl)vinyl anion equivalent to the derived Weinreb amide.¹⁰⁵ Felkin-Anh selective ketone reduction and silylation of the so-formed 2°-alcohol was followed by cyclisation by Pd(0)-mediated *O*-allylation to give the *anti,syn*-oxazine diastereomer **179** (Scheme 33). This sequence (steps a–g) had been reported and exploited previously by the authors. In order to introduce the C(7a) stereogenic centre, Grignard addition to the aldehyde obtained by alkene ozonolysis was tested under a variety of conditions. In the absence of external additives, low *syn/anti*-ratios were obtained but in the presence of a slight excess of $ZnCl_2$ the addition of butenyl magnesium bromide formed essentially one diastereomer, consistent with reaction at the less hindered aldehyde face in a conformation fixed by chelation to the oxazine ring oxygen. After mesylation and *N*-protection, intermediate **180** was cyclised by *N*-alkylation and reductive amination steps to give the target alkaloid in fifteen steps overall.

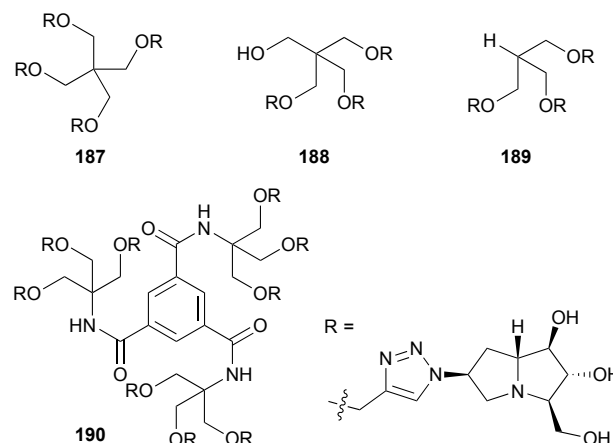


Scheme 33 Reagents and conditions: (a) PhCOCl, Et₃N, CH₂Cl₂; (b) TBSCl, imidazole, DMF; (c) (MeO)NHMe·HCl, Me₃Al, CH₂Cl₂; (d) (E)-Bu₃SnCH=CHCH₂Cl, MeLi, THF, −78 °C; (e) LiAlH(Ot-Bu)₃, EtOH, −78 °C; (f) TBSCl, imidazole, DMF; (g) NaH, Pd(PPh₃)₄, TBAI, THF, 0 °C; (h) O₃, MeOH, −78 °C then Me₂S; (i) but-3-en-1-yl-MgBr, ZnCl₂, THF, −78 °C; (j) MsCl, Et₃N, CH₂Cl₂, 0 °C; (k) CbzCl, NaHCO₃, aq. CH₂Cl₂; (l) NaH, THF; (m) O₃, MeOH, −78 °C then Me₂S; (n) H₂, Pd(OH)₂, MeOH; (o) HCl, aq. MeOH, reflux [→ *ent*-149·HCl] then Dowex 40W X8.

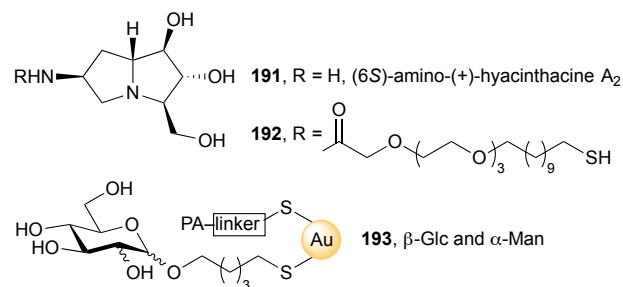
Goti reported an application of the group's well-developed nitron cycloaddition / reductive amination strategy to the hyacinthacine B analogue **182** from **181**, derived from L-xylose or D-arabinose.¹⁰⁶ This compound showed 95% inhibition of *Aspergillus niger* amyloglucosidase at 1 mM (IC₅₀ = 39 μM). Nitron cycloaddition followed by reductive amination was also used to give four C(5)-methyl hyacinthacine analogues **183–186**.¹⁰⁷



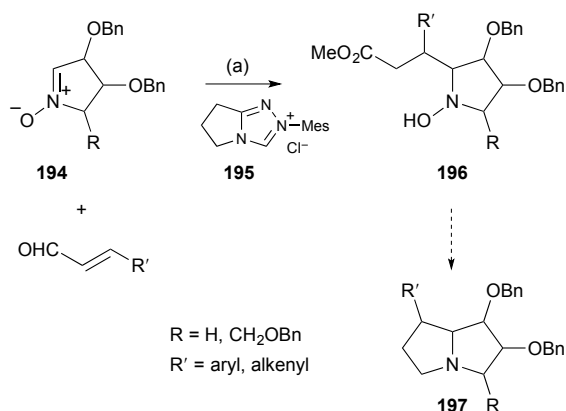
Goti and Cardona also used this strategy to access (6S)-azidoxyhyacinthacine A₂.¹⁰⁸ This azide was then combined with a variety of symmetrical branched polyalkynes by multiple click cycloadditions to give 'multivalent pyrrolizidine' analogues **187–190**. These molecules were tested for inhibitory activity against eight different glycosidases. All showed effective inhibition of *Aspergillus niger* amyloglucosidase at 1 mM (IC₅₀ = 0.7–1.6 μM). Lower level selective inhibition of bovine kidney α-L-fucosidase, coffee bean α-galactosidase, yeast α-glucosidase, and jack bean α-mannosidase was also found.



From the same key azide, the group prepared and acylated amine **191**, producing thiol **192**.¹⁰⁹ This was then immobilised at two different 'densities' (20% and 40%) onto gold glyconanoparticles (Au-GNPs) adorned with either β-glucosyl or α-mannosyl chains **193**. The four iminosugar Au-GNPs exhibited low micromolar inhibition of the amyloglucosidase from *Aspergillus niger* with the higher density pair having a higher IC₅₀. The authors' work supports the view that increasing the multivalency of iminosugars does not necessarily result in increased bioactivity.

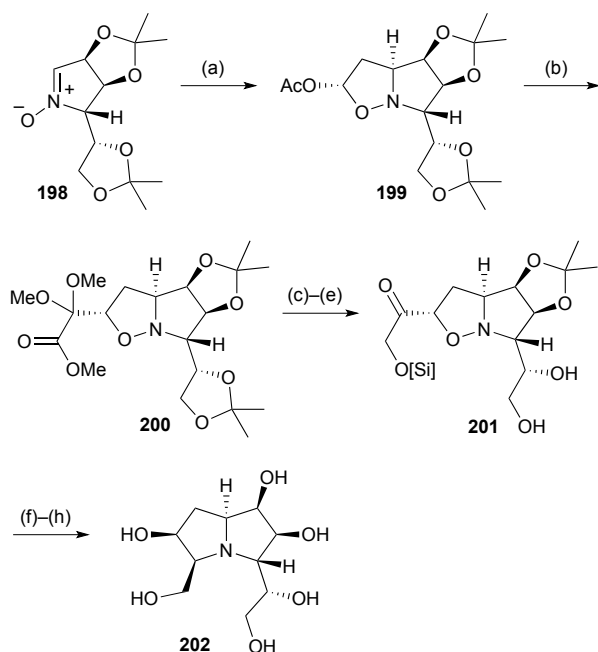


Kato and Yu reported the organocatalysed reaction of sugar-derived nitrones with 3-alkenyl or 3-aryl enals to give functionalised pyrrolidines of the form **196** (Scheme 34).¹¹⁰ Mediated by the pre-catalyst **195** the aldehydes connect at C(3) to the nitron **194** pro-C(7a) position from the face *anti*-to the adjacent benzyloxy substituent. During the process, internal proton transfer results in overall oxidation of the aldehyde carbon so that ejection of the catalyst by the nitron oxygen affords a lactone which is cleaved by methanolysis at the end of the reaction. These intermediates were then reduced and cyclised to give a variety of C(7)-alk(en)yl/aryl substituted PAs **197**. The authors reported 16 relevant examples with one of these converted into (7R)-phenylhyacinthacine A₂.^{110a} a parallel Chinese patent lists many more examples.^{110b}



Scheme 34 Reagents and conditions: (a) DBU, CH_2Cl_2 , $0^\circ\text{C} \rightarrow \text{rt}$ then NaOMe, MeOH.

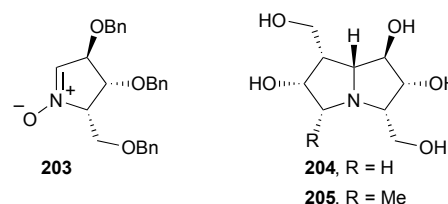
In a further elaboration of sugar-derived nitrones, Fischer's group developed a synthesis of a hyacinthacine C_2 analogue **202** (Scheme 35) in which the C(7) hydroxy group in the natural product is moved to C(6) and the C(3) hydroxymethyl substituent is homologated.¹¹¹ The adduct **199** between vinyl acetate and nitrone **198**, from mannose, undergoes loss of acetate in the presence of TMSOTf as Lewis acid, and trapping follows from the *exo*-face of the so-formed oxonium ion by a glyoxal equivalent (step b). The resulting protected α -ketoester **200** was then taken through a series of reduction and protecting group manipulation steps to generate the PA homologue **202** in a concise overall sequence.



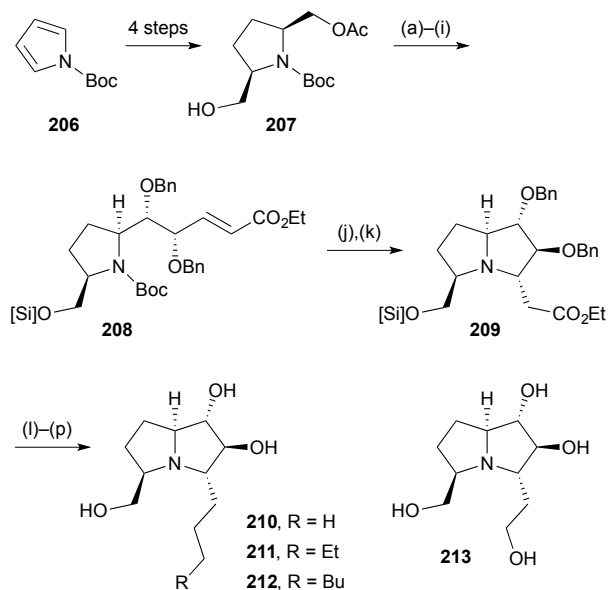
Scheme 35 Reagents and conditions: (a) vinyl acetate, 75°C [dr = 87:13]; (b) $(\text{MeO})_2\text{C}=\text{C}(\text{OTMS})\text{OMe}$, TMSOTf, CH_2Cl_2 , -80°C ; (c) LiAlH_4 , THF, 0°C ; (d) TBDPSCI, imidazole, CH_2Cl_2 ; (e) aq. AcOH, 60°C ; (f) H_2 , Pd/C, EtOH; (g) TBAF, THF; (h) aq. TFA then Dowex (H^+ form). [Si] = TBDPS.

Carbohydrate-derived nitrone **203** was the starting point in routes to the two non-natural pyrrolizidines **204** and **205** that were evaluated for their ability to inhibit a panel of

glycosidases.¹¹² The 5-methyl-containing compound **205** was active only against coffee bean α -galactosidase ($\text{IC}_{50} = 68.0 \mu\text{M}$) but the less substituted compound **204** was both more active for this enzyme ($\text{IC}_{50} = 5.4 \mu\text{M}$) and showed activity against bovine liver β -galactosidase ($\text{IC}_{50} = 82.9 \mu\text{M}$).



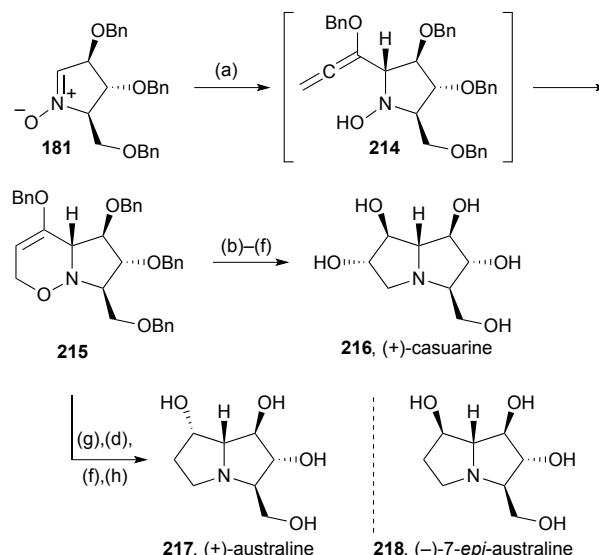
Based on the occurrence in *Scilla* species of hydroxylated pyrrolizidines bearing extended side chains at C(5), Toyooka's group developed routes to non-natural hyacinthacine analogues with extended C(3) substituents and tested their glycosidase inhibition.¹¹³ The monoacetate $(-)-(2S,5R)$ -**207** (Scheme 36) was prepared from *N*-Boc pyrrole **206** by double carboxylation, two reductive steps, then enzymatic acylation with CAL-B/vinyl acetate. Protecting group and redox manipulation steps were followed by HWE reaction, dihydroxylation, and a second HWE olefination to provide intermediate **208**. Removal of the Boc protecting group initiated aza-Michael addition, thought to proceed kinetically via a conformation that avoids steric clashing between the $\text{CH}_2\text{O}[\text{Si}]$ and developing $\text{CH}_2\text{CO}_2\text{Et}$ substituents. Ester reduction and cleavage of the benzyl protecting groups generated analogue **213**; alternatively, partial ester reduction then Wittig reaction and reduction produced the three C(3)-alkyl analogues **210–212**. These four pyrrolizidines, plus their enantiomers, were evaluated for inhibition of seven glycosidases. Hydroxyethyl analogue **213** showed moderate, selective inhibition of α -L-fucosidase from bovine kidney; most analogues, in both series, inhibited β -galactosidase from bovine liver.



Scheme 36 Reagents and conditions: (a) TBDPSCI, imidazole, CH_2Cl_2 ; (b) K_2CO_3 , MeOH; (c) SO_3 , pyridine, Et_3N , DMSO; (d) $(\text{EtO})_2\text{PO}\cdot\text{CH}_2\text{CO}_2\text{Et}$, NaH, THF; (e) OsO_4 , NMO, aq. acetone [dr ~ 2:1]; (f) NaH, BnBr, DMF; (g) LiBH_4 , THF; (h) Dess–Martin periodinane, CH_2Cl_2 ; (i) $(\text{EtO})_2\text{PO}\cdot\text{CH}_2\text{CO}_2\text{Et}$, NaH, THF; (j) $\text{CF}_3\text{CO}_2\text{H}$, CH_2Cl_2 ; (k) K_2CO_3 , CH_2Cl_2 ; (l) DIBAL, CH_2Cl_2 , -78°C ; (m) $\text{Ph}_3\text{P}^+\text{CH}_2\text{R}^-\text{X}^-$, $t\text{-BuOK}$, THF; (n) H_2 , Pd/C, EtOAc; (o) TBAF, THF; (p) BCl_3 , THF. [Si] = TBDPS.

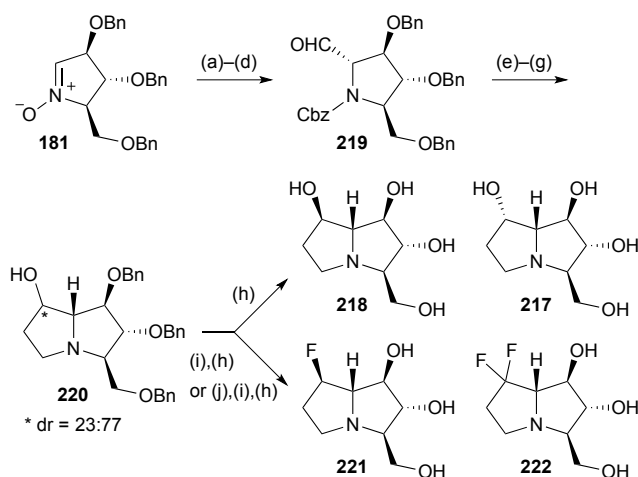
Casuarines and australines

Prior to the publication of the synthesis of a simple tetrahydroxy pyrrolizidine (Scheme 25), Reissig and Goti had disclosed the strategy in the context of the preparation of three PAs related by the same stereochemistry at C(1–3) and C(7a).¹¹⁴ Here, nitron **181** gave, via adduct **214** (Scheme 37), cyclisation product **215**, a common intermediate for the synthesis of (+)-casuarine **216**, (+)-australine **217** and its epimer at C(7) **218**. Thus, hydroboration and oxidation produced the C(6)–C(7) *trans*-diol motif present in (+)-casuarine **216**, the synthesis being completed by N–O reduction, cyclisation *via* the mesylate, and deprotection. Alternatively, from **215**, performing these last steps first led to the australine core bearing a C(7)-carbonyl; reduction of this ketone afforded (+)-australine **217** with complete stereoselectivity resulting from hydride delivery from the *exo*-face. A modification of the sequence to casuarine, including C(6)-deoxygenation by vigorous DIBAL reduction of the mesylate, gave access to (–)-7-*epi*-australine **218**. This last PA showed 95% inhibition of *Aspergillus niger* amyloglucosidase at 1 mM ($\text{IC}_{50} = 3.5\ \mu\text{M}$).



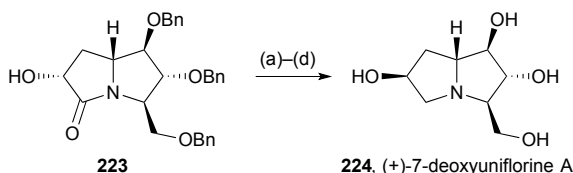
Scheme 37 Reagents and conditions: (a) (benzyloxy)allene, BuLi, THF, -78°C then Na_2SO_4 , CH_2Cl_2 , rt; (b) $\text{BH}_3\cdot\text{THF}$, THF then H_2O_2 , aq. NaOH; (c) Zn, aq. AcOH, 65°C or SmI_2 , THF; (d) MsCl , Et_3N , CH_2Cl_2 ; (e) LiAlH_4 , THF, reflux; (f) H_2 , Pd/C, aq. HCl, MeOH; (g) $\text{Mo}(\text{CO})_6$, NaBH₄, aq. CH_3CN , reflux; (h) NaBH₄, MeOH.

Nitron **181** (Scheme 38) was converted into a mixture of pyrrolizidine diastereomers **220**, epimeric at C(7) with the β -isomer being major.¹¹⁵ Hydrogenolysis of the benzyl ethers gave (–)-7-*epi*-australine **218** and (+)-australine **217**. DAST-mediated fluorination of either of the diastereomers of **220** resulted, after deprotection, in the production of the same β -configured 7-fluoro-7-deoxyaustraline derivative **221**; the authors speculate that neighbouring group participation by the nitrogen atom intervenes, at least in the case of β -**220** where substitution proceeds with clean retention of configuration. Treating the ketone derived from alcohol **220** with DAST led to the 7,7-difluorinated australine analogue **222** after benzyl hydrogenolysis; in the difluorination step a tricyclic compound (not shown) was produced in ~40% yield by cyclisation of the CH_2OBn oxygen at C(3) onto C(7). The same four end products were prepared in the enantiomeric series from *ent*-**181**, derived from D-xylose. Evaluation of the eight australine variants ability to inhibit a range of glycosidases was also undertaken. The *ent*-**217**, **218**, **221**, **222** variants were essentially inactive in all assays; (+)-australine **217**, its 7-epimer **218**, and the C(7)-difluoro analogue **222** were effective inhibitors of *Aspergillus niger* α -glucosidase and amyloglucosidase; the C(7)-monofluoro compound **221** was ~10 times as effective as (+)-australine in its inhibition of *A. niger* α -glucosidase ($\text{IC}_{50} = 0.63\ \mu\text{M}$) and also showed reasonable activity against porcine kidney trehalase.



Scheme 38 Reagents and conditions: (a) $\text{H}_2\text{C}=\text{CHMgBr}$, THF, 0 °C; (b) Zn, AcOH; (c) CbzCl, NaHCO_3 , aq. THF; (d) ozonolysis; (e) Zn, allyl bromide, NH_4Cl , aq. THF; (f) O_3 , MeOH, -60 °C then Me_2S ; (g) H_2 , Pd/C, AcOH, MeOH; (h) H_2 , Pd/C, HCl, aq. MeOH; (i) DAST, pyridine, CH_2Cl_2 , 0 °C (\rightarrow **221**) or rt (\rightarrow **222**); (j) $(\text{COCl})_2$, DMSO, CH_2Cl_2 , -40 °C then Et_3N .

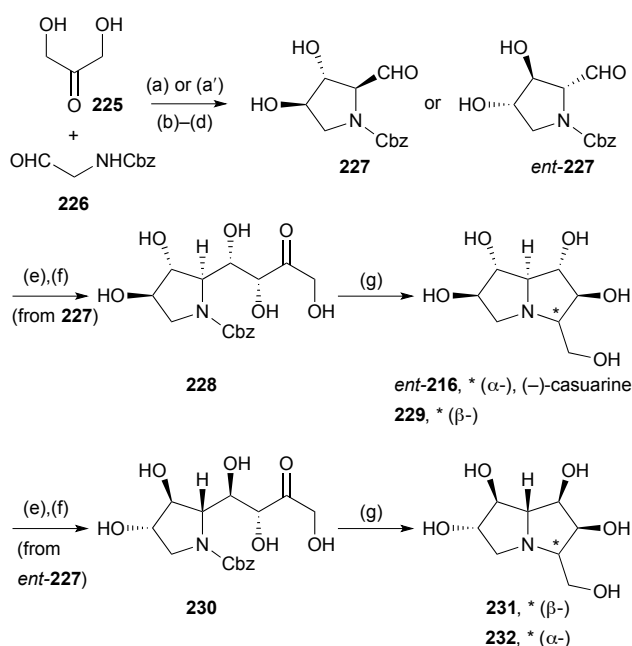
Pyrrolizidinone **223** (Scheme 39), whose preparation from nitron **181** was described in the previous review, was inverted at C(6) then reduced to give (+)-dexoyuniflorine A **224**.¹¹⁶ This, and three further pyrrolizidines [(−)-uniflorine A, 7-deoxycasuarine, and 7-deoxy-6-(α -glucopyranosyl)casuarine] showed little inhibition of α -amylase (from human saliva), little or comparatively weak activity against porcine trehalase, but moderate to high nanomolar inhibition of insect trehalases from *Chironomus riparius*, and *Spodoptera littoralis*. The authors concluded that such selective activity holds promise for the future development of insecticides.



Scheme 39 Reagents and conditions: (a) $p\text{-NO}_2\text{C}_6\text{H}_4\text{CO}_2\text{H}$, DIAD, PPh_3 , THF; (b) Ambersep 900 OH, MeOH; (c) LiAlH_4 , THF, reflux; (d) H_2 , Pd/C, HCl, MeOH then Dowex 50WX8-200.

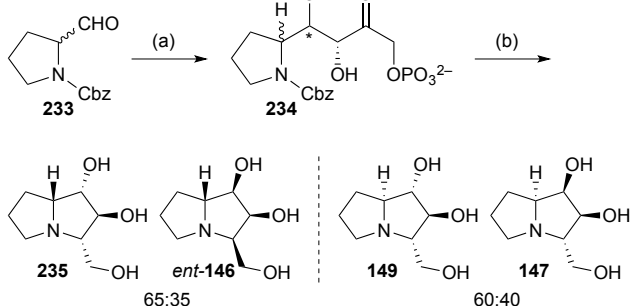
Further applications of Clapés' chemoenzymatic synthesis of highly oxygenated PAs from dihydroxyacetone **225** are summarised in Scheme 40 which shows stereodivergent routes to *ent*-casuarine **216**, its 3-epimer **229**, and both 2-*epi*- and 2,3-di-*epi*-casuarine, **231** and **232**, respectively.¹¹⁷ These alkaloids were screened for glycosidase activity against bakers yeast α -glucosidase, rice α -glucosidase, and *Penicillium decumbens* α -rhamnosidase. The most promising compound (**229**) strongly inhibited rice α -glucosidase ($\text{IC}_{50} = 7.9 \pm 5.2 \mu\text{M}$) and, in follow up, also showed activity against rat intestinal sucrase ($\text{IC}_{50} = 3.5 \pm 0.6 \mu\text{M}$) and rat intestinal maltase ($\text{IC}_{50} = 39 \pm 13 \mu\text{M}$).

A separate paper reports the synthesis of a variety of 5,6-annulated (benzo-, cyclohexano-) hydroxy-PA derivatives.¹¹⁸



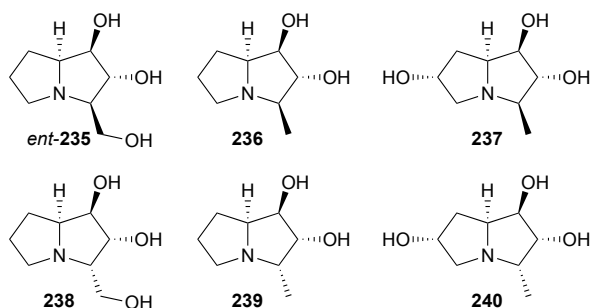
Scheme 40 Reagents and conditions: (a) $\text{FSA}^{\text{A129S/A165G}}$; (a') RhuA; (b) H_2 , Pd/C; (c) Cbz-OSu, aq. dioxane; (d) IBX, EtOAc, reflux; (e) DHAP, FucA^{F131A}, aq. DMF; (f) acid phosphatase, pH 5; (g) H_2 , Pd/C, aq. MeOH then ion exchange chromatography (CM-Sephacrose- NH_4^+).

More recently, the group described the use of L-rhamnulose-1-phosphate aldolase from *Thermotoga maritima* (Rhu1PATm) to prepare four hyacinthacine isomers *ent*-**146**, **147**, **149**, and **235** (Scheme 41). There is some ambiguity in the stereochemistry of these pyrrolizidines; the depicted structure for **147** reflects the name provided in the experimental section, rather than that presented in Scheme 4 of the paper (which is the 1,3-diepimer).¹¹⁹



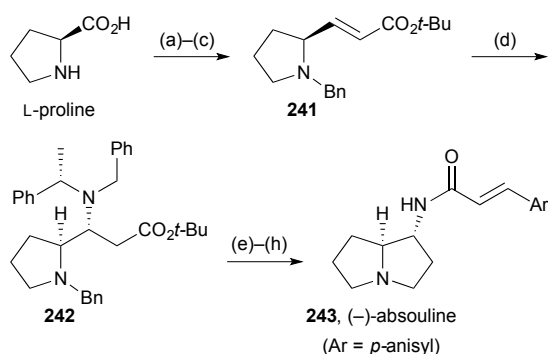
Scheme 41 Reagents and conditions: (a) DHAP, Rhu1PATm, aq. DMF then potato acid phosphatase, aq. HCl; (b) H_2 , Pd/C, aq. MeOH.

Pyrrolizidines *ent*-**235** and **236–240** were prepared by a similar two step process.¹²⁰



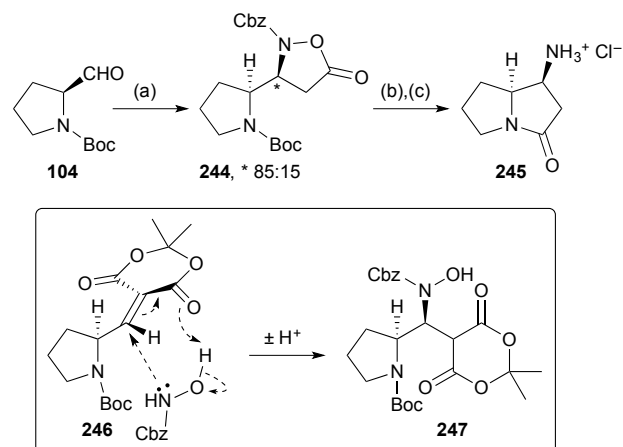
Aminopyrrolizidines

Davies' synthesis¹²¹ of the non-natural (–)-enantiomer of absoulone **243** (Scheme 42) is strategically similar to that reported by Scheerer's group, summarised in the previous review. The advance in Davies' version is the use of the chiral ammonia equivalent lithium (*S*)-*N*-benzyl-*N*-(α -methylbenzyl)amide to control the stereochemistry at C(1) (step d). From adduct **242**, hydrogenolysis of all benzylic linkages and subsequent lactam formation and reduction led to (1*R*,7*aS*)-1-aminopyrrolizidine; acylation with *p*-methoxycinnamic acid completed the synthesis, in eight steps overall and 20% yield.



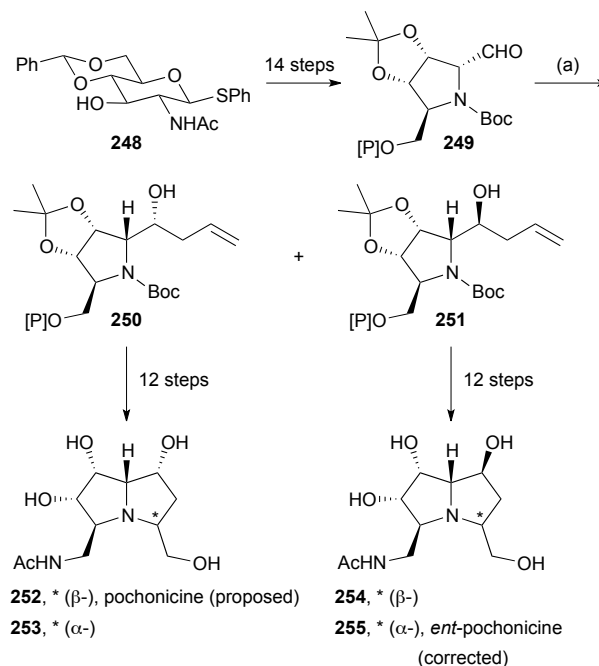
Scheme 42 Reagents and conditions: (a) PhCOCl , aq. NaOH , 0 °C; (b) LiAlH_4 , THF, reflux; (c) $(\text{COCl})_2$, DMSO, Et_3N , CH_2Cl_2 , –78 °C then $\text{Ph}_3\text{P=CHCO}_2\text{t-Bu}$, CH_2Cl_2 ; (d) lithium (*S*)-*N*-benzyl-*N*-(α -methylbenzyl)amide, THF, –78 °C; (e) H_2 , $\text{Pd}(\text{OH})_2/\text{C}$, aq. HCl , MeOH ; (f) aq. HCl , 90 °C; (g) DIBAL , THF, 0 °C \rightarrow rt; (h) *trans*- $\text{ArCH=CHCO}_2\text{H}$, DCC, DMAP, CH_2Cl_2 , 0 °C \rightarrow rt.

Brière's group developed a three component synthesis of isoxazolidinones from an aldehyde, an *N*-alkylhydroxylamine or alkyl hydroxycarbamate, and Meldrum's acid.¹²² With aldehydes bearing an α -heteroatom, *syn*-diastereoselectivity was observed. This methodology was applied to a short synthesis of (*S,S*)-1-aminopyrrolizidinone **245** (Scheme 43). Thus, the *syn*-1,2-diamino functionality in intermediate **244** was established by condensation with *N*-Boc (*S*)-prolinal **104** and aza-Michael addition of benzyl hydroxycarbamate (via **246** and **247**). Hydrogenolysis of the N–O bond and CBz group in isoxazolidinone **244**, followed by acid treatment, gave lactam **245**, a known precursor to 1-aminopyrrolizidines.



Scheme 43 Reagents and conditions: (a) Meldrum's acid, benzyl hydroxycarbamate, DABCO, pyrrolidine, EtOAc ; (b) H_2 , Pd/C , *i*- PrOH , 60 °C; (c) aq. HCl , 90 °C.

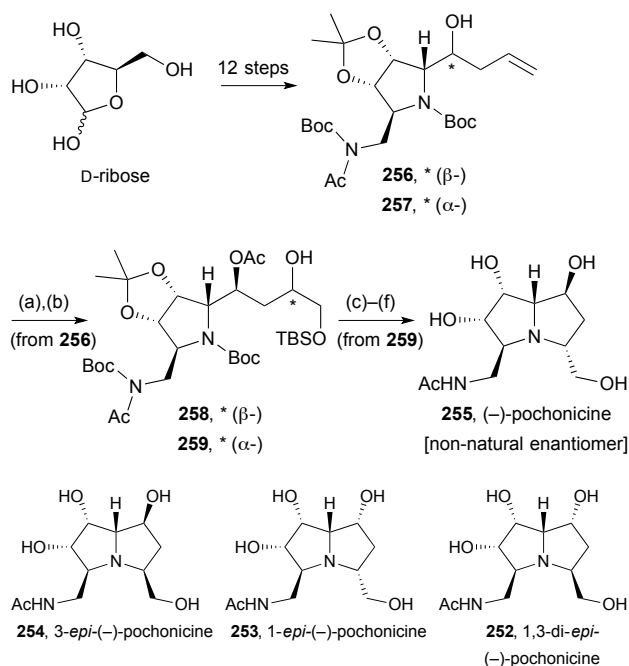
Takahashi reported a synthesis of the structure **252** proposed for (+)-pochonicine (Scheme 44).¹²³ The tetrasubstituted *N*-Boc-pyrrolidine derivative **249** was prepared from *N*-acetylglucosamine and allylated to give a roughly 3:1 ratio of diastereomers **250** and **251**. The major isomer **250** was taken on to the proposed (+)-pochonicine. During the route, alkene dihydroxylation was not fully selective; therefore, cyclisation *via* the mesylate provided both C(3) epimers (**252** and **253**). Neither diastereomer showed spectroscopic data matching the literature values for the natural product. From the minor allylated isomer **251**, the same sequence generated C(3) epimers **254** and **255**. The NMR spectroscopic data epimer **255** matched those reported for the natural product but the specific rotation was of opposite sign; accordingly, the structure of (+)-pochonicine is revised to *ent*-**255**.



Scheme 44 Reagents and conditions: (a) allyl-MgCl, ZnCl_2 , CH_2Cl_2 , THF, –78 °C [dr = 77:23]. [Si] = TBDPS.

This structural reassignment was subsequently confirmed by Kato and Yu who prepared the same set of diastereomers plus their enantiomers from D-ribose or L-ribose, in an overall more concise route.¹²⁴ In essence, the synthesis was strategically the same as Takahashi's, with stereochemical branching points at the allylation (\rightarrow C(1)-epimers **256/257**, Scheme 45) and dihydroxylation (\rightarrow C(3)-epimers, **258/259**) stages.

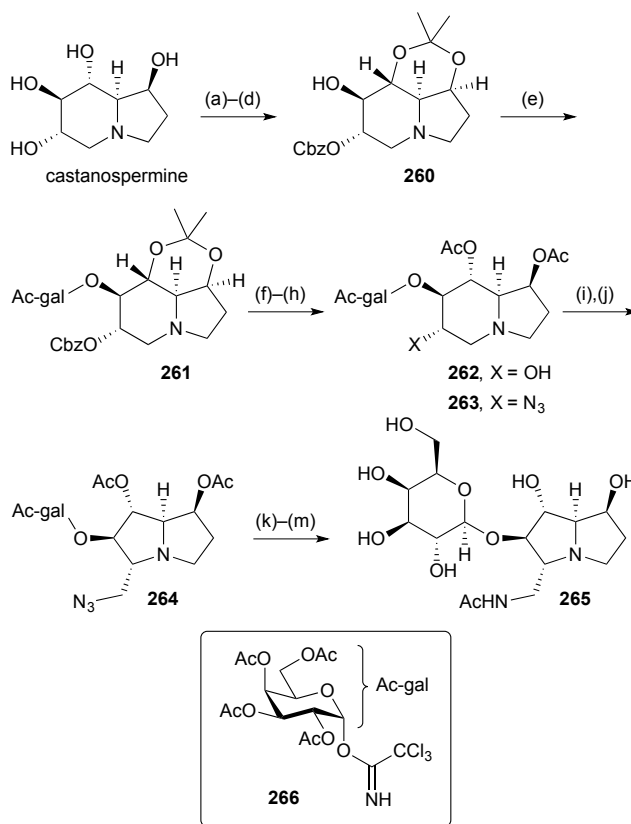
In both the Takahashi and Kato–Yu syntheses, the glycosidase inhibitory properties of the various pochonicine isomers were evaluated. (–)-Pochonicine (the non-natural enantiomer) was found to be around 10,000 times weaker than the (+)-enantiomer in inhibiting jack bean *N*-acetylglucosaminidase.¹²³ Whilst pochonicine showed significant inhibition of a panel of glycosidases¹²⁴ the IC₅₀ values were somewhat less impressive than those reported in the original isolation paper.



Scheme 45 Reagents and conditions: (a) OsO₄, NMO, aq. acetone [dr = 1.2:1]; (b) TBSCl, Et₃N, DMAP, CH₂Cl₂; (c) MsCl, Et₃N, CH₂Cl₂; (d) Zn, Br₂, *p*-cresol; (e) K₂CO₃, MeOH; (f) aq. HCl, MeOH.

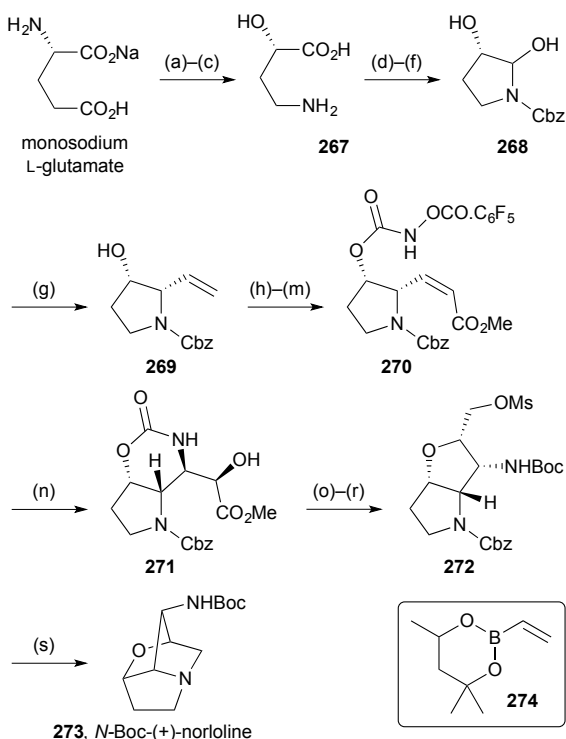
In a research programme aimed at understanding the role of lacto-*N*-biosidase (LNBase), an enzyme that releases lacto-*N*-biose from human milk oligosaccharides, Stubbs prepared a series of amino- and iminosugars and glycosylated -izidines as potential LNBase inhibitors.¹²⁵ One of these **265** (Scheme 46) was prepared from castanospermine starting with a series of protecting group manipulations that left a single free hydroxy group in derivative **260**. A 2,3,4,6-tetra-*O*-acetyl-β-galactosyl group was introduced relatively early on in the sequence via trichloroacetimidate **266** (step e). Azide displacement of the mesylate derived from alcohol **262** gave mainly the castanospermine derivative **263** along with a significant amount of the ring-contracted 5-azidomethylpyrrolizidine **264**, structurally related to pochonicine (Scheme 45). Deprotection and purification steps afforded the potential inhibitor **265**. This

small molecule inhibited the LNBase from *Bifidobacterium bifidum* ($K_i = 52 \pm 2 \mu\text{M}$) but it was the weakest of the six compounds tested and about 10 times less potent than the castanospermine variant derived from **263**.



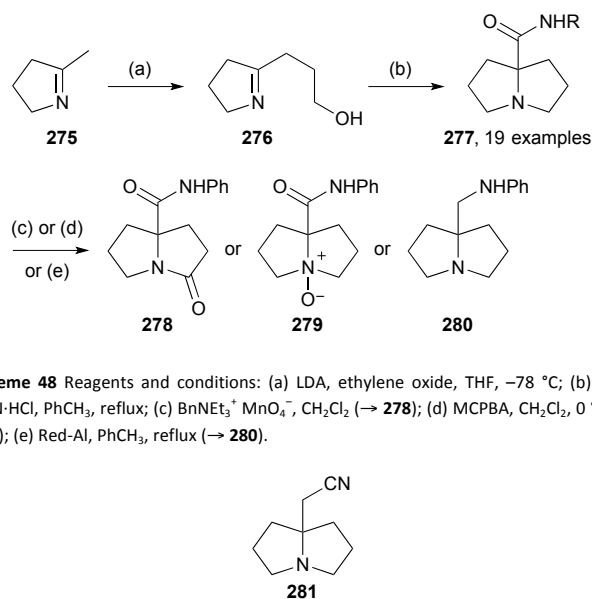
Scheme 46 Reagents and conditions: (a) PhCOCl, pyridine; (b) 2-methoxypropene, TsOH·H₂O, DME, 55 °C; (c) NaOMe, MeOH; (d) CbzCl, Et₃N, THF; (e) **266**, TMSOTf, 4 Å MS, CH₂Cl₂, –30 °C to rt; (f) aq. AcOH, 70 °C; (g) Ac₂O, pyridine; (h) H₂, Pd/C, MeOH; (i) MsCl, pyridine, 0 °C to rt; (j) NaN₃, DMSO [\rightarrow **263**, 27% and **264**, 15%]; (k) H₂, Pd/C, MeOH; (l) Ac₂O, pyridine; (m) NaOMe, MeOH then AG50W-X4 (H⁺), H₂O.

Scheerer reported a second generation route to the loline alkaloid system (Scheme 47).¹²⁶ There are strategic similarities with the first generation route (described in the previous review) but the more recent route provides enantiopure material from L-glutamic acid and access to the Z-alkenyl side chain is achieved more directly by Petasis boronic acid Mannich reaction (step g \rightarrow **269**) then RCM (step i). In this new route, the tethered aminohydroxylation was also optimised and the pentafluorobenzyloxy carbamate, in combination with an enoate (step n \rightarrow **271**), shown to be much more efficient than the original simple carbamate coupled with an allylic alcohol. The route then followed an analogous sequence to that developed earlier for the racemate. Here, ester reduction, double mesylation, and Boc-activation of the oxazinanone enabled cleavage of the imide to be effected exclusively at the endocyclic carbonyl. Cyclisation of the so-formed 2°-hydroxy group gave bicyclic intermediate **272** that cyclised to the norloline derivative **273** upon hydrogenolysis of the Cbz group. Overall, the synthesis is a similar length to the first generation route but is significantly more efficient and provides multi-milligram quantities for further study.



Scheme 47 Reagents and conditions: (a) NaNO_2 , aq. HCl, 0 °C to 10 °C; (b) NH_3 , EtOH; (c) Cl_2 , aq. NaOH, 50 °C; (d) HMDS, TMSCl, PhCH_3 , reflux then EtOH; (e) LHMS, CbzCl, THF, -78 °C then aq. HCl; (f) NaBH_4 , MeOH, 0 °C; (g) **274**, $\text{BF}_3\cdot\text{OEt}_2$, CH_2Cl_2 , -78 °C to rt; (h) acryloyl chloride, *i*- Pr_2NEt , DMAP, CH_2Cl_2 , -78 °C to rt; (i) Hoveyda–Grubbs II (Hoveyda–Bleichert catalyst), DCE, reflux; (j) $\text{LiOH}\cdot\text{H}_2\text{O}$, aq. THF; (k) MeI, K_2CO_3 , DMF; (l) $\text{NH}_2\text{OH}\cdot\text{HCl}$, CDI, pyridine, 0 °C to rt; (m) $\text{C}_6\text{F}_5\text{COCl}$, Et_3N , CH_2Cl_2 , 0 °C; (n) $\text{K}_2\text{OsO}_4\cdot\text{H}_2\text{O}$, aq. *t*-BuOH; (o) LiBH_4 , THF, 0 °C; (p) MsCl, pyridine; (q) Boc_2O , DMAP, THF; (r) Cs_2CO_3 , MeOH; (s) H_2 , $\text{Pd}(\text{OH})_2$, MeOH.

In closing this section, two short syntheses of non-natural 7a-aminoalkyl pyrrolidines have been reported. The first involves an interesting transformation of 2-hydroxypropyl pyrroline **276** (Scheme 48).¹²⁷ Presumably, Ritter-type addition of the isocyanide to the protonated pyrroline, is followed by capture of the nitrilium ion by the tethered hydroxy group; evolution of the so-formed cyclic imidate to the pyrrolizidine system may be mediated by the chloride ion present in the reaction which can act as a nucleophilic catalyst in a ring-opening/ring-closure sequence. Nineteen varied amides **277** were produced by this methodology and the *N*-phenyl amide ($\text{R} = \text{Ph}$) used to exemplify three redox transformations to give **278–280**. Separately, a process for preparing a precursor **281** to homologues of amines of the form **280** was disclosed.¹²⁸

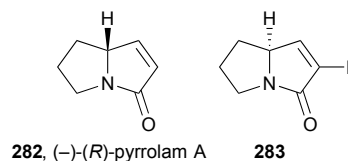


Scheme 48 Reagents and conditions: (a) LDA, ethylene oxide, THF, -78 °C; (b) RNC, $\text{Et}_3\text{N}\cdot\text{HCl}$, PhCH_3 , reflux; (c) $\text{BnNEt}_3^+ \text{MnO}_4^-$, CH_2Cl_2 (\rightarrow **278**); (d) MCPBA, CH_2Cl_2 , 0 °C (\rightarrow **279**); (e) Red-Al, PhCH_3 , reflux (\rightarrow **280**).

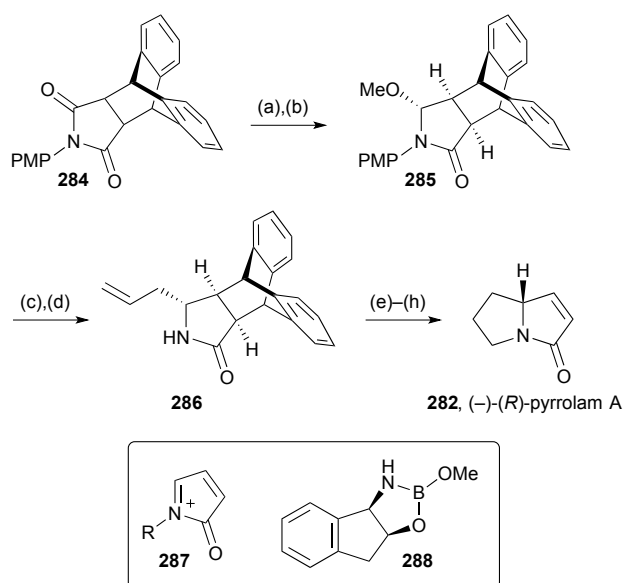
Pyrrolams, hydroxydanaidone

The product of organocatalytic amination of 5-(*tert*-butyldimethylsilyl)oxypentanal **125** (Scheme 23) was taken through a similar sequence to provide (–)-(*R*)-pyrrolam A **282** and pyrrolizidine (hexahydro-1*H*-pyrrolizine, not shown).¹²⁹

A short RCM route from *N*-Boc-(2*S*)-vinylpyrrolidine (from (*S*)-proline in three steps) and 2-fluoroacryloyl chloride gave access to fluoropyrrolam A derivative **283**.¹³⁰

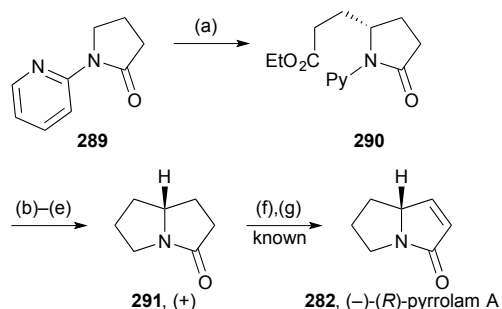


The second synthesis of (–)-(*R*)-pyrrolam A during the review period employed a chiral equivalent of iminium ion **287** (Scheme 49).¹³¹ The strategy was based on protection of the enone double bond of maleimide as a Diels–Alder adduct with anthracene which also served to maintain the absolute stereochemistry during the production and trapping of the iminium centre. In the forward direction, asymmetric borohydride reduction catalysed by oxazaborolidine **288** provided methoxylactam **285** (99% ee) after formation of the aminal from the intermediate hemiaminal. Iminium formation and allylation then *N*-deprotection afforded *exo*-allyllactam **286** as a single diastereomer. From this point the synthesis followed conventional lines with flash vacuum pyrolysis releasing the target molecule in the final step; this compound is known to racemise readily but just a slight erosion in enantiomeric purity was found in this instance (**282**, 94% ee).



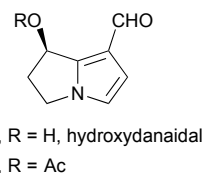
Scheme 49 Reagents and conditions: (a) **288** (10 mol%), $\text{BH}_3 \cdot \text{THF}$, THF [ee = 99%]; (b) TsOH , MeOH, 60°C ; (c) allyl-SiMe₃, $\text{BF}_3 \cdot \text{OEt}_2$, CH_2Cl_2 , $-78^\circ\text{C} \rightarrow \text{rt}$; (d) CAN, aq. CH_3CN , $0^\circ\text{C} \rightarrow \text{rt}$; (e) $\text{BH}_3 \cdot \text{THF}$, THF, $0^\circ\text{C} \rightarrow \text{rt}$ then H_2O_2 , aq. NaOH; (f) MsCl , Et_3N , DMAP, CH_2Cl_2 , -10°C ; (g) DBU, EtOH, reflux; (h) 490°C (FVP).

Shibata has developed the use of an *N*-(2-pyridyl) group to direct enantioselective C–H activation and alkylation with alkenes. Scheme 50 illustrates an application of this to the formal synthesis of (–)-(*R*)-pyrrolam A.¹³² The initial alkylation (step a) was slow, taking one week in boiling dioxane to reach completion, but the product **290** was produced in high yield with a 90% ee. This level of enantiomeric purity was retained during the following four steps that comprised removal of the 2-pyridyl group, ester reduction and tosylation, then base-mediated cyclisation. In the paper, the product **291** is mis-drawn but may be inferred to be that shown here based on retention of stereochemistry from lactam **290**. The route stopped at this point but the final steps (f and g) are known.



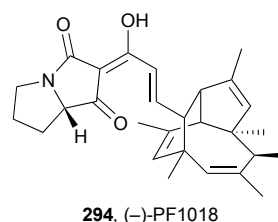
Scheme 50 Reagents and conditions: (a) ethyl acrylate, $[\text{Ir}(\text{cod})_2]\text{BF}_4$, (*R*)-tolBINAP, dioxane, reflux; (b) H_2 , $\text{Pd}(\text{OH})_2/\text{C}$, HCl, EtOH; (c) LiAlH_4 , MeOH; (d) TsCl , Et_3N , DMAP, CH_2Cl_2 ; (e) NaH, THF; (f) LDA, PhSeCl , THF, -78°C ; (g) H_2O_2 , aq. NaOH.

Glasnov published an efficient microwave mediated hydrolysis of monocrotaline to produce retronecine which was oxidised selectively to give hydroxydanaidal **292** and its *O*-acetyl derivative **293**.¹³³ Hydrogenation of retronecine under various pressures of H_2 under continuous flow conditions gave mixtures of desoxyretronecine, retronecanol, and platynecine.

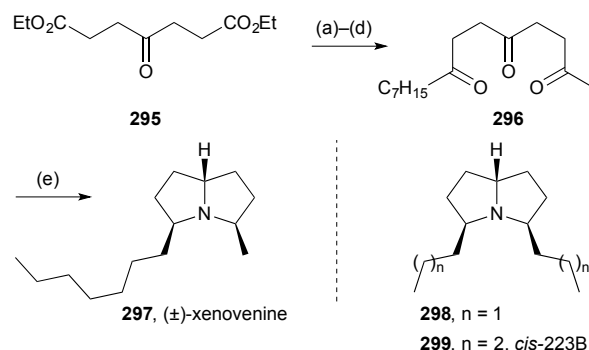


Miscellaneous¹³⁴

Trauner described progress towards the total synthesis of the unusual polyketide (–)-PF1018 **294** isolated from a fungal *Humicola* sp. strain, that contains a pyrrolizidine-1,3-dione side chain.¹³⁵ The synthetic chemistry focused on the tricyclic hydrocarbon moiety, prepared by an elegant 8π -electrocyclisation and Diels–Alder cascade.



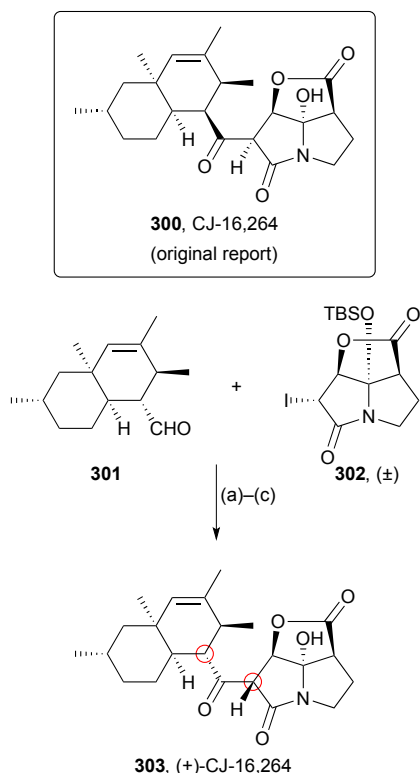
Stockman prepared racemic xenovenine **297** (from the ant *Solenopsis xenovenum*), alkaloid *cis*-223B **299** (originally from the toad *Melanophryniscus stelzneri*) and its dipropyl analogue **298** (Scheme 51) by a 'bioinspired' triple reductive amination of appropriate tricarbonyl precursors.¹³⁶ Under the optimised conditions shown (step e), the alkaloids were produced as single diastereomers, an outcome originally envisaged by the authors as resulting from thermodynamic control.



Scheme 51 Reagents and conditions: (a) ethylene glycol, PPTS, PhCH_3 , reflux; (b) $\text{NH}(\text{OMe})\text{Me}$, *i*-PrMgCl, THF, $-15^\circ\text{C} \rightarrow \text{rt}$; (c) $\text{C}_7\text{H}_{15}\text{MgBr}$ then MeMgBr , THF, $-60^\circ\text{C} \rightarrow \text{rt}$; (d) aq. HCl; (e) NH_4OAc , NaBH_3CN , MeOH.

Nicolaou conducted a synthesis of candidate stereoisomers of the antibiotic CJ-16,264 because its close relatives (pyrrolizilactone, UCS1025A, and UCS1025B) have different stereochemistry, particularly in the pyrrolizidinone part of the molecule, which is enantiomeric.¹³⁷ This work resulted in a correction to the relative stereochemistry from **300** (Scheme 52) and assigned the absolute stereochemistry for the (+)-enantiomer as that shown in **303**, the differing stereogenic centres being circled in the revised structure. Diastereomers of aldehyde **301**, prepared from either (*R*)- or (*S*)-citronellol, were coupled with racemic iodopyrrolizidinone **302** to generate,

after desilylation and 2°-alcohol oxidation, six candidate structures. By comparison of spectroscopic and specific rotation data, the correct structure could be assigned with confidence.

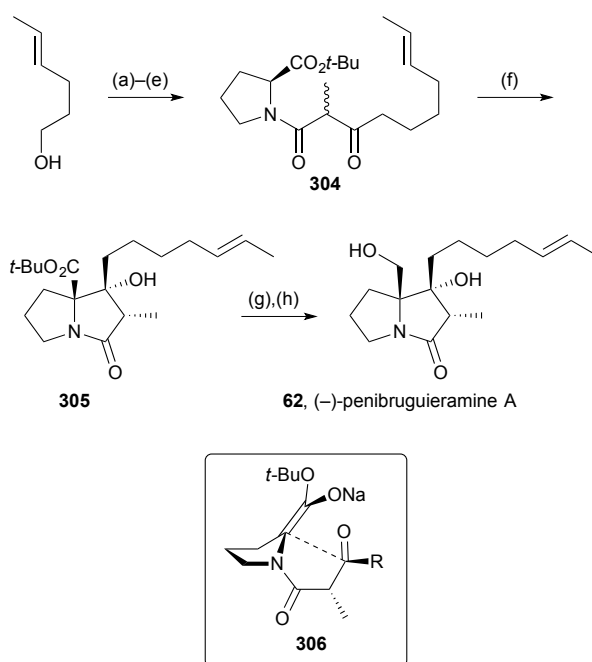


Scheme 52 Reagents and conditions: (a) Et_3B , PhCH_3 , -78°C ; (b) tris(dimethylamino)sulfoniumdifluoro trimethylsilicate, THF, 0°C ; (c) Dess–Martin periodinane, CH_2Cl_2 .

(–)-Penibruquieramine A, recently isolated as described earlier,⁷¹ was synthesised in a route based on its proposed biosynthesis from ketoamide **63**.¹³⁸ The *tert*-butyl ester of the enantiomer of this ketoamide **304** (Scheme 53) was prepared in five steps from *E*-hex-4-en-1-ol via enolate displacement of the derived 1°-alkyl bromide then coupling with (*S*)-proline as its *tert*-butyl ester. The key step in this route (step f) involved intramolecular aldol cyclisation which afforded pyrrolizidinone **305** as a single diastereomer in high yield, remarkable given the weak base and protic solvent employed for this transformation; see below for a mechanistic discussion. Reduction of the *tert*-butyl ester gave material spectroscopically identical to the natural product with an ee in excess of 99%; the structure (of **305**) was further confirmed by X-ray crystallography.

A series of mechanistic investigations shed light on the cyclisation, in particular its stereochemical course: (1) performing the reaction to partial completion in EtOD showed incorporation of deuterium at all acidic positions both in the product and the recovered starting material; (2) subjecting the separated epimers of **304** (at the methyl-bearing ketoamide centre) to the cyclisation conditions showed equilibration to a 1.4:1 mixture of methyl- α and methyl- β isomers (with reference to the structure in Scheme 53) within 10 minutes,

then conversion to the cyclised product **305** took place slowly, over ~ 10 hours. On the basis of these observations, the authors concluded that all acidic sites are rapidly and reversibly deprotonated *including the stereogenic proline α -centre* and cyclisation takes place through a conformation **306** in which allylic strain is minimised in the minor epimer at equilibrium. The cyclisation step, therefore, employs both memory of chirality and dynamic kinetic resolution; the product was also shown, by computation, to be the most stable stereoisomer.



Scheme 53 Reagents and conditions: (a) MsCl , Et_3N , THF; (b) LiBr , THF, reflux; (c) ethyl 2-methylacetoacetate, NaH , BuLi ; (d) KOH , aq. MeOH ; (e) (*S*)-proline *tert*-butyl ester, DCC , DMAP , CH_2Cl_2 ; (f) NaOEt , EtOH ; (g) $\text{CF}_3\text{CO}_2\text{H}$, CH_2Cl_2 ; (h) benzotriazoloxyl-tris(dimethylamino)phosphonium hexafluorophosphate, *i*- Pr_2NEt , THF then NaBH_4 .

Outlook

Since their first discovery and characterisation as toxic components in plants the PAs have fascinated researchers across diverse fields of study and continue to do so. The published research summarised herein represents a mere fraction of the activity being undertaken in hundreds of laboratories and field studies worldwide with new developments appearing weekly. In looking back over the recent literature, a few highlights emerge: (1) The importance of the bacterial pyrrolizidines as a class will no doubt increase rapidly now that the genes responsible for their biosynthesis have been characterised and observed in diverse species. (2) A broader approach to assaying PAs for biological activity should be rewarded with new starting points for drug development. (3) A growing awareness of the presence of toxic PAs in herbal preparations means that steps can be taken to minimise chronic exposure and reduce illness whose cause is currently potentially unknown. (4) Synthetic chemists should be inspired

by some of the very concise and efficient routes that are becoming more frequent, realise that chiral pool starting points may well offer tempting 'free' stereochemistry but often lead to lengthy sequences, and continue to consider PAs as valid targets for stimulating creative new strategies.

References

- J. Robertson and K. Stevens, *Nat. Prod. Rep.* 2014, **31**, 1721.
- M. M. Fashe, R. O. Juvonen, A. Petsalo, J. Vepsäläinen, M. Pasanen and M. Rahnasto-Rilla, *Chem. Res. Toxicol.* 2015, **28**, 702.
- M. M. Fashe, R. O. Juvonen, A. Petsalo, J. Räsänen and M. Pasanen, *Chem. Res. Toxicol.* 2015, **28**, 2034.
- See reference 1, p1732.
- Q. Xia, Y. Zhao, L. S. Von Tungeln, D. R. Doerge, G. Lin, L. Cai and P. P. Fu, *Chem. Res. Toxicol.* 2013, **26**, 1384.
- Y. Zhao, S. Wang, Q. Xia, G. G. da Costa, D. R. Doerge, L. Cai and P. P. Fu, *Chem. Res. Toxicol.* 2014, **27**, 1720.
- X. Jiang, S. Wang, Y. Zhao, Q. Xia, L. Cai, X. Sun and P. P. Fu, *J. Food Drug Anal.* 2015, **23**, 318.
- Q. Xia, L. Ma, X. He, L. Cai and P. P. Fu, *Chem. Res. Toxicol.* 2015, **28**, 615.
- M. M. Fashe, R. O. Juvonen, A. Petsalo, M. Rahnasto-Rilla, S. Auriola, P. Soininen, J. Vepsäläinen and M. Pasanen, *Chem. Res. Toxicol.* 2014, **27**, 1950.
- R. A. Field, B. L. Stegelmeier, S. M. Colegate, A. W. Brown and B. T. Green, *Toxicon* 2015, **97**, 36.
- A. Xiong, F. Yang, L. Fang, L. Yang, Y. He, Y. Y.-J. Wan, Y. Xu, M. Qi, X. Wang, K. Yu, K. W.-K. Tsim and Z. Wang, *Chem. Res. Toxicol.* 2014, **27**, 775.
- J. Tang, Z. Wang, T. Akao and M. Hattori, *Nat. Prod. Commun.* 2013, **8**, 1545.
- J. Ruan, C. Liao, Y. Ye and G. Lin, *Chem. Res. Toxicol.* 2014, **27**, 7.
- T. Beuerle, I. Mädege and L. Cramer, *Deut. Lebensm.-Rundsch.* 2014, **110**, 241.
- <http://www.bfr.bund.de/cm/349/pyrrolizidine-alkaloids-in-herbal-teas-and-teas.pdf> [accessed July 2016].
- M. Opatowska, C. T. Elliott, A.-C. Huet, M. McCarthy, P. P. J. Mulder, C. von Holst, P. Delahaut, H. P. Van Egmond and K. Campbell, *Anal. Bioanal. Chem.* 2014, **406**, 757.
- C. T. Griffin, M. Danaher, C. T. Elliott, D. G. Kennedy and A. Furey, *Food Chem.* 2013, **136**, 1577.
- M. Martinello, C. Cristofoli, A. Gallina and F. Mutinelli, *Food Control* 2014, **37**, 146.
- L. C. Bretanha, M. Piovezan, A. F. V. Sako, M. G. Pizzolatti and G. A. Micke, *Amer. J. Anal. Chem.* 2014, **5**, 681.
- F. J. Orantes-Bermejo, J. S. Bonvehí, A. Gómez-Pajuelo, M. Megías and C. Torres, *Food. Addit. Contam.: Part A* 2013, **30**, 1799.
- C. Lu, T. Ding, X. Ma, G. Chen, F. Yang, B. Wu, C. Shen, R. Zhang, X. Fei, X. Zhang, L. Chen and L. Li, *Chin. J. Chromatogr.* 2013, **31**, 1046.
- E. M. Mudge, A. Maxwell, P. Jones and P. N. Brown, *Food Addit. Contam.: Part A* 2015, **32**, 2068.
- T. Griffin, S. M. Mitrovic, M. Danaher and A. Furey, *Food Addit. Contam.: Part A* 2015, **32**, 214.
- H. Neumann and A. Huckauf, *J. Verbr. Lebensm.* 2015, **10**; DOI 10.1007/s00003-015-0986-0.
- Y. Cao, S. M. Colegate and J. A. Edgar, *J. Food. Comp. Anal.* 2013, **29**, 106.
- L. Cramer, H.-M. Schiebel, L. Ernst and T. Beurle, *J. Agric. Food. Chem.* 2013, **61**, 11382.
- L. Zhu, J.-Q. Ruan, N. Li, P. P. Fu, Y. Ye and G. Lin, *Food. Chem.* 2016, **194**, 1320.
- C. Allgaier and S. Franz, *Regul. Toxicol. Pharmacol.* 2015, **73**, 494.
- B. Avula, S. Sagi, Y.-H. Wang, J. Zweigenbaum, M. Wang and I. A. Khan, *Food Chem.* 2015, **178**, 136.
- C.-H. Hsieh, H.-W. Chen, C.-C. Lee, B.-J. He and Y.-C. Yang, *J. Food Comp. Anal.* 2015, **42**, 1.
- C. F. Bosi, D. W. Rosa, R. Grougnet, N. Lemonakis, M. Halabalaki, A. L. Skaltsounis and M. W. Biavatti, *Braz. J. Pharmacogn.* 2013, **23**, 425.
- C. Mathon, P. Edler, S. Bieri and P. Christen, *Anal. Bioanal. Chem.* 2014, **406**, 7345.
- T. Desta, M. Afework, C. R. Unnithan and H. Alay, *Int. J. Pharm. Tech.* 2014, **6**, 6281.
- C. T. Griffin, F. Gosetto, M. Danaher, S. Sabatini and A. Furey, *Food. Addit. Contam.: Part A* 2014, **31**, 940.
- M. Schulz, J. Meins, S. Diemert, P. Zagermann-Muncke, R. Goebel, D. Schrenk, M. Schubert-Zsilavecz and M. Abdel-Tawab, *Phytomed.* 2015, **22**, 648.
- I. Mädege, L. Cramer, I. Rahaus, G. Jerz, P. Winterhalter and T. Beuerle, *Food Chem.* 2015, **187**, 491.
- A. Shimshoni, A. Duebecke, P. P. J. Mulder, O. Cuneah and S. Barel, *Food Addit. Contam.: Part A* 2015, **32**, 2058.
- L. Cramer, G. Fleck, G. Horn and T. Beurle, *J. Am. Oil Chem. Soc.* 2014, **91**, 721.
- G. Vacillotto, D. Favretto, R. Seraglia, R. Pagiotti, P. Traldi and Luisa Mattoli, *J. Mass. Spectrom.* 2013, **48**, 1078.
- D. Bodi, S. Ronczka, C. Gottschalk, N. Behr, A. Skibba, M. Wagner, M. Lahrssen-Wiederholt, A. Preiss-Weigert and A. These, *Food Addit. Contam.: Part A* 2014, **31**, 1886.
- B. Huybrechts and A. Callebaut, *Food Addit. Contam.: Part A* 2015, **32**, 1939.
- J. Becerra-Jimenez, M. Kuschak, E. Roeder and H. Wiedenfeld, *Pharmazie* 2013, **68**, 636.
- C. Gottschalk, S. Ronczka, A. Preiß-Weigert, J. Ostertag, H. Klaffke, H. Schafft and M. Lahrssen-Wiederholt, *Animal Feed Sci. Technol.* 2015, **207**, 253.
- M. Bolechová, J. Čáslavský, M. Pospíchalová and P. Kosubová, *Food Chem.* 2015, **170**, 265.
- M. de Nijs, I. J. W. Elbers and P. P. J. Mulder, *Food. Addit. Contam.: Part A* 2014, **31**, 288.
- S. H. Yoon, M.-S. Kim, S. H. Kim, H. M. Park, H. Pyo, Y. M. Leed, K.-T. Lee and J. Hong, *J. Chromatogr. B* 2015, **992**, 56.
- B. M. Mandić, M. D. Vlajić, S. S. Trifunović, M. R. Simić, L. V. Vujisić, I. M. Vučković, M. M. Novaković, S. D. Nikolić-Mandić, V. V. Tešević, V. V. Vajs and S. M. Milosavljević, *Nat. Prod. Res.* 2015, **29**, 887.
- A. Schenk, B. Siewert, S. Toff. and J. Drewe, *J. Chromatogr. B* 2015, **997**, 23.
- E. Cairns, M. A. Hashmi, A. J. Singh, G. Eakins, M. Lein and R. Keyzers, *J. Agric. Food Chem.* 2015, **63**, 7421.
- B. Tasso, F. Novelli, F. Sparatore, F. Fasoli and C. Gotti, *J. Nat. Prod.* 2013, **76**, 727.
- B. M. Mandić, M. R. Simić, I. M. Vučković, L. V. Vujisić, M. M. Novaković, S. S. Trifunović, S. D. Nikolić-Mandić, V. V. Tešević, V. V. Vajs and S. M. Milosavljević, *Molecules* 2013, **18**, 10694.
- P. Appadurai and K. Rathinasamy, *Toxicol. Lett.* 2014, **225**, 66.
- S. S. Kusuma, K. Tanneeru, S. Didla, B. N. Devendra and P. Kiranmayi, *Anti-cancer Agents Med. Chem.* 2014, **14**, 1237.
- A. Kato, Y. Hirokami, K. Kinami, Y. Tsuji, S. Miyawaki, I. Adachi, J. Hollinshead, R. J. Nash, J. L. Kiappes, N. Zitzmann, J. K. Cha, R. J. Molyneux, G. W. J. Fleet and N. Asano, *Phytochem.* 2015, **111**, 124.

- 55 D. A. C. Bezerra, J. F. Tavares, P. F. dos Santos, M. V. S. C. Branco, M. de Fátima Agra, F. L. Subrinho, R. Braz-Filho and M. S. da Silva, *Magn. Reson. Chem.* 2013, **51**, 497.
- 56 S. M. Colegate, D. R. Gardner, T. Z. Davis, J. M. Betz and K. E. Panter, *Phytochem. Anal.* 2013, **24**, 201.
- 57 H. Damianakos, G. Sotiroudis and I. Chinou, *J. Nat. Prod.* 2013, **76**, 1829.
- 58 Q.-H. Sun, J.-J. Yang, X.-H. Wei, H. Xu and G.-X. Chou, *Phytochem. Lett.* 2013, **6**, 449.
- 59 S. Huang, X.-l. Zhou, C.-j. Wang, Y.-s. Wang, F. Xiao, L.-h. Shan, Z.-y. Guo and J. Weng, *Phytochem.* 2013, **93**, 154.
- 60 C. Villanueva-Cañongo, N. Pérez-Hernández, B. Hernández-Carlos, E. Cedillo-Portugal, P. Joseph-Nathan and E. Burgueño-Tapia, *Magn. Reson. Chem.* 2014, **52**, 251.
- 61 B. M. Fraga, C. E. Díaz, L. J. Amador, Matias Reina, O. Santana and A. González-Coloma, *Phytochem.* 2014, **108**, 220.
- 62 M. Boppré and S. M. Colegate, *Phytochem. Anal.* 2015, **26**, 215.
- 63 S. M. Colegate, M. Boppré, J. Monzón and J. M. Betz, *J. Ethnopharmacol.* 2015, **172**, 179.
- 64 L. S. Hoang, M. H. Tran, J. S. Lee, D. C. To, V. T. Nguyen, J. A. Kim, J. H. Lee, M. H. Woo and B. S. Min, *Chem. Pharm. Bull.* 2015, **63**, 481.
- 65 J. Pan, M. Bhardwaj, J. R. Faulkner, P. Nagabhyru, N. D. Charlton, R. M. Higashi, A.-F. Miller, C. A. Young, R. B. Grossman and C. L. Schardl, *Phytochem.* 2014, **98**, 60.
- 66 T. Nogawa, M. Kawatani, M. Uramoto, A. Okano, H. Aono, Y. Futamura, H. Koshino, S. Takahashi and H. Osada, *J. Antibiot.* 2013, **66**, 621.
- 67 R. Sugiyama, S. Nishimura and H. Kakeya, *Tetrahedron Lett.* 2013, **54**, 1531.
- 68 P. Yu, A. Patel and K. N. Houk, *J. Am. Chem. Soc.* 2015, **137**, 13518.
- 69 W. Zhang, S. Li, Y. Zhu, Y. Chen, Y. Chen, H. Zhang, G. Zhang, X. Tian, Y. Pan, S. Zhang, W. Zhang and C. Zhang, *J. Nat. Prod.* 2014, **77**, 388.
- 70 D. K. Derewacz, B. C. Covington, J. A. McLean and B. O. Bachmann, *ACS Chem. Biol.* 2015, **10**, 1998.
- 71 Z.-F. Zhou, T. Kurtán, X.-H. Yang, A. Mándi, M.-Y. Geng, B.-P. Ye, O. Taglialatela-Scafati and Y.-W. Guo, *Org. Lett.* 2014, **16**, 1390.
- 72 L. M. Petersen, J. C. Frisvad, P. B. Knudsen, M. Røhlfs, C. H. Gotfredsen and T. O. Larsen, *J. Antibiot.* 2015, **68**, 603.
- 73 S. Huang, J. Tabudravu, S. S. Elsayed, J. Travert, D. Peace, M. H. Tong, K. Kyeremeh, S. M. Kelly, L. Trembleau, R. Ebel, M. Jaspars, Y. Yu and H. Deng, *Angew. Chem. Int. Ed.* 2015, **54**, 12697.
- 74 O. Schimming, V. L. Challinor, N. J. Tobias, H. Adihou, P. Grün, L. Pöschel, C. Richter, H. Schwalbe and H. B. Bode, *Angew. Chem. Int. Ed.* 2015, **54**, 12702.
- 75 P. Fu and J. B. MacMillan, *Org. Lett.* 2015, **17**, 3046.
- 76 M. C. Kim, J. H. Lee, B. Shin, L. Subedi, J. W. Cha, J.-S. Park, D.-C. Oh, S. Y. Kim and H. C. Kwon, *Org. Lett.* 2015, **17**, 5024.
- 77 Review: M. Brambilla, S. G. Davies, A. M. Fletcher and J. E. Thomson, *Tetrahedron: Asymmetry* 2014, **25**, 387.
- 78 D. Koley, K. Srinivas, Y. Krishna and A. Gupta, *RSC Adv.* 2014, **4**, 3934.
- 79 M. Brambilla, S. G. Davies, A. M. Fletcher, P. M. Roberts and J. E. Thomson, *Tetrahedron* 2014, **70**, 204.
- 80 N. A. Sorto, M. J. Di Maso, M. A. Muñoz, R. J. Dougherty, J. C. Fetting and J. T. Shaw, *J. Org. Chem.* 2014, **79**, 2601.
- 81 S. G. Davies, A. M. Fletcher, E. M. Foster, I. T. T. Houlsby, P. M. Roberts, T. M. Schofield and J. E. Thomson, *Org. Biomol. Chem.* 2014, **12**, 9223.
- 82 J. Li, H. Zhao, X. Jiang, X. Wang, H. Hu, Lei Yu and Y. Zhang, *Angew. Chem. Int. Ed.* 2015, **54**, 6306.
- 83 K. B. Gavhane, S. B. Bhorkade and M. G. Kulkarni, *Tetrahedron: Asymmetry* 2015, **26**, 746.
- 84 D. W. Knight, A. C. Share and P. T. Gallagher, *J. Chem. Soc., Perkin Trans. 1* 1997, 2089.
- 85 I. Chogii and J. T. Njardarson, *Angew. Chem. Int. Ed.* 2015, **54**, 13706.
- 86 D. J. Aldous, A. S. Batsanov, D. S. Yufit, A. J. Dalençon, W. M. Dutton and P. G. Steel, *Org. Biomol. Chem.* 2006, **4**, 2912.
- 87 C. Heescher, D. Schollmeyer and U. Nubbemeyer, *Eur. J. Org. Chem.* 2013, 4399.
- 88 E. Zapata-Machin, T. Castellan, C. Baudoin-Dehoux and Y. Génisson, *Synth. Commun.* 2015, **45**, 635.
- 89 S. Du-a-man, D. Soorukram, C. Kuhakarn, P. Tuchinda, V. Reutrakul and M. Pohmakotr, *Eur. J. Org. Chem.* 2014, 1708.
- 90 S. V. Kauloorkar, V. Jha, G. Jogdand and P. Kumar, *Org. Biomol. Chem.* 2014, **12**, 4454.
- 91 K. R. Luna-Freire, J. P. S. Scaramal, J. A. L. C. Resende, C. F. Tormena, F. L. Oliveira, R. Aparicio and F. Coelho, *Tetrahedron* 2014, **70**, 3319.
- 92 M. Jasinski, E. Moreno-Clavijo and H.-U. Reissig, *Eur. J. Org. Chem.* 2014, 442.
- 93 P. Rajasekaran, A. A. Ansari and Y. D. Vankar, *Eur. J. Org. Chem.* 2015, 2902.
- 94 S. Basu, P. S. Kandiya, R. S. Ampapathi and T. K. Chakraborty, *RSC Adv.* 2013, **3**, 13630.
- 95 A. Rajender, J. P. Rao and B. V. Rao, *Eur. J. Org. Chem.* 2013, 1749.
- 96 E. A. Brock, S. G. Davies, J. A. Lee, P. M. Roberts and J. E. Thomson, *Org. Biomol. Chem.* 2013, **11**, 3187.
- 97 P. V. Reddy, J. Smith, A. Kamath, H. Jamet, A. Veyron, P. Koos, C. Philouze, A. E. Greene and P. Delair, *J. Org. Chem.* 2013, **78**, 4840.
- 98 J. Smith, A. Kamath, A. E. Greene and P. Delair, *Synlett* 2014, **25**, 209.
- 99 A. Veyron, P. V. Reddy, P. Koos, A. Bayle, A. E. Greene and P. Delair, *Tetrahedron: Asymmetry* 2015, **26**, 85.
- 100 J. Marjanovic, V. Divjakovic, R. Matovic, Z. Ferjancic and R. N. Saicic, *Eur. J. Org. Chem.* 2013, 5555.
- 101 R. Lahiri, Y. S. Reddy, S. A. Kulkarni and Y. D. Vankar, *RSC Adv.* 2013, **3**, 23242.
- 102 K. Savasun, C. W. G. Au and S. G. Pyne, *J. Org. Chem.* 2014, **79**, 4569.
- 103 C.-M. Si, Z.-Y. Mao, R.-G. Ren, Z.-T. Du and B.-G. Wei, *Tetrahedron* 2014, **70**, 7936.
- 104 M. Bergeron-Brelek, M. Meanwell and R. Britton, *Nature Commun.* 2015, **6**, 6903.
- 105 S.-H. Park, X. Jin, J.-C. Kang, C. Jung, S.-S. Kim, S.-S. Kim, K.-Y. Lee and W.-H. Ham, *Org. Biomol. Chem.* 2015, **13**, 4539.
- 106 D. Martella, F. Cardona, C. Parmeggiani, F. Franco, J. A. Tamayo, I. Robina, E. Moreno-Clavijo, A. J. Moreno-Vargas and A. Goti, *Eur. J. Org. Chem.* 2013, 4047.
- 107 P. Gkizis, N. G. Argyropoulos and E. Coutouli-Argyropoulou, *Tetrahedron* 2013, **69**, 8921.
- 108 G. D'Adamio, C. Parmeggiani, A. Goti, A. J. Moreno-Vargas, E. Moreno-Clavijo, I. Robina and F. Cardona, *Org. Biomol. Chem.* 2014, **12**, 6250.
- 109 C. Matassini, M. Marradi, F. Cardona, C. Parmeggiani, I. Robina, A. J. Moreno-Vargas, S. Penadés and A. Goti, *RSC Adv.* 2015, **5**, 95817.
- 110 (a) W.-Y. Xu, R. Iwaki, Y.-M. Jia, W. Zhang, A. Kato and C.-Y. Yu, *Org. Biomol. Chem.* 2013, **11**, 4622; (b) C. Yu, W. Xu, Y. Jia, W. Zhang and Z. She, CN 103467470 A, 2013.
- 111 D. Benadiková, M. Medvecký, A. Filipová, J. Moncol, M. Gembický, N. Prónayová and R. Fischer, *Synlett* 2014, **25**, 1616.

- 112R. Lahiri, A. Palanivel, S. A. Kulkarni and Y. D. Vankar, *J. Org. Chem.* 2014, **79**, 10786.
- 113D. Minehira, T. Okada, R. Iwaki, A. Kato, I. Adachi, N. Toyooka, *Tetrahedron Lett.* 2015, **56**, 331.
- 114C. Parmeggiani, F. Cardona, L. Giusti, H.-U. Reissig and A. Goti, *Chem. Eur. J.* 2013, **19**, 10595.
- 115Y.-X. Li, Y. Shimada, K. Sato, A. Kato, W. Zhang, Y.-M. Jia, G. W. J. Fleet, M. Xiao and C.-Y. Yu, *Org. Lett.* 2015, **17**, 716.
- 116G. D'Adamio, A. Sgambato, M. Forcella, S. Caccia, C. Parmeggiani, M. Casartelli, P. Parenti, D. Bini, L. Cipolla, P. Fusi and F. Cardona, 2015, *Org. Biomol. Chem.* 2015, **13**, 886.
- 117A. L. Concia, L. Gómez, T. Parella, J. Joglar and P. Clapés, *J. Org. Chem.* 2014, **79**, 5386.
- 118P. Laborda, F. J. Sayago, C. Cativiela, T. Parella, J. Joglar and P. Clapés, *Org. Lett.* 2014, **16**, 1422.
- 119 I. Oroz-Guinea, K. Hernández, F. C. Bres, C. Guérard-Hélaine, M. Lemaire, P. Clapés and E. García-Junceda, *Adv. Synth. Catal.* 2015, **357**, 1951.
- 120A. Soler, M. L. Gutiérrez, J. Bujons, T. Parella, C. Minguillon, J. Joglar and P. Clapés, *Adv. Synth. Catal.* 2015, **357**, 1787.
- 121S. G. Davies, A. M. Fletcher, C. Lebé, P. M. Roberts, J. E. Thomson and J. Yin, *Tetrahedron* 2013, **69**, 1369.
- 122C. Berini, M. Sebban, H. Oulyadi, M. Sanselme, V. Levacher and J.-F. Brière, *Org. Lett.* 2015, **17**, 5408.
- 123Y. Kitamura, H. Koshino, T. Nakamura, A. Tsuchida, T. Nitoda, H. Kanzaki, K. Matsuoka and S. Takahashi, *Tetrahedron Lett.* 2013, **54**, 1456.
- 124J.-S. Zhu, S. Nakagawa, W. Chen, I. Adachi, Y.-M. Jia, X.-G. Hu, G. W. J. Fleet, F. X. Wilson, T. Nitoda, G. Horne, R. van Well, A. Kato and C.-Y. Yu, *J. Org. Chem.* 2013, **78**, 10298.
- 125M. Hattie, T. Ito, A. W. Debowski, T. Arakawa, T. Katayama, K. Yamamoto, S. Fushinobud and K. A. Stubbs, *Chem. Commun.* 2015, **51**, 15008.
- 126K. E. Miller, A. J. Wright, M. K. Olesen, M. T. Hovey and J. R. Scheerer, *J. Org. Chem.* 2015, **80**, 1569.
- 127I. P. Kerschgens and K. Gademann, *Synthesis* 2015, **47**, 3153.
- 128C. Lu, P. Zeng, M. Sun and X. Gu, CN 104311561 (2015).
- 129S. V. Kauloorkar, V. Jha and P. Kumar, *RSC Adv.* 2013, **3**, 18288.
- 130M. Marhold, C. Stillig, R. Fröhlich and G. Haufe, *Eur. J. Org. Chem.* 2014, 5777.
- 131B. J. Marsh, H. Adams, M. D. Barker, I. U. Kutama and S. Jones, *Org. Lett.* 2014, **16**, 3780.
- 132Y.-K. Tahara, M. Michino, M. Ito, K. S. Kanyivab and T. Shibata, *Chem. Commun.* 2015, **51**, 16660.
- 133S. T. Martinez, A. C. Pinto, T. Glasnov and C. O. Kappe, *Tetrahedron Lett.* 2014, **55**, 4181.
- 134Review of the synthesis of a variety of -izidine alkaloids from proline: C. Bhat and S. G. Tilve, *RSC Adv.* 2014, **4**, 5405.
- 135R. Webster, B. Gaspar, P. Mayer and D. Trauner, *Org. Lett.* 2013, **15**, 1866.
- 136A. Barthelme, D. Richards, I. R. Mellor and R. A. Stockman, *Chem. Commun.* 2013, **49**, 10507.
- 137K. C. Nicolaou, A. A. Shah, H. Korman, T. Khan, L. Shi, W. Worawalai and E. A. Theodorakis, *Angew. Chem. Int. Ed.* 2015, **54**, 9203.
- 138J. H. Kim, S. Lee and S. Kim, *Angew. Chem. Int. Ed.* 2015, **54**, 10875.